Mathematics

https://www.aimspress.com/journal/Math

AIMS Mathematics, 11(8): 26986–27017.
DOI: 10.3934/math.20261082
Received: 02 July 2026
Revised: 08 August 2026
Accepted: 17 August 2026
Published: 27 August 2026

Research article

Numerical stability analysis of a class of nonlinear age-structured tumor cell population models

Hefan Yin[1], **Jianfang Gao**[1,2,*], **and Zhanwen Yang**[3]

[1] School of Mathematical Sciences, Harbin Normal University, Harbin 150025, China

[2] Heilongjiang Key Laboratory of Analysis on Machine Learning and Dynamic System, Harbin Normal University, Harbin 150025, China

[3] School of Mathematics, Harbin Institute of Technology, Harbin 150001, China

* **Correspondence:** Email: 09151108@163.com.

Abstract: A nonlinear age-structured tumor cell population model where the tumor population is divided into proliferating and quiescent cells is studied in this paper. The discretization of age and time is considered. Based on continuous collocation methods, an age-semi-discrete scheme and the numerical basic reproduction number R_h are obtained. Some conditions are presented such that R_h is superconvergent to the real basic reproduction number R_0, and R_h is also a threshold of the age-semi-discrete scheme. For the time-full discretization, an implicit-explicit discrete scheme is introduced, of which the computational cost is almost the same as an explicit scheme. The most important point is that the dynamical behavior of the model is preserved by the age-semi-discrete scheme. Finally, several numerical experiments are given to verify our results.

Keywords: age-structured; proliferating and quiescent cells; continuous collocation methods; numerical basic reproduction number; stability
Mathematics Subject Classification: 65M12, 65M70, 65M15

1. Introduction

Cell population models were first proposed by Bell and Anderson [1,2], who investigated the effects of cell division into daughter cells of unequal volumes and derived conditions for the existence and stability of a balanced exponential solution. However, cells can also be described by many other state variables besides volume, such as age [3, 4], size [5], and spatial location [6, 7]. Recent studies have also employed delayed, fractional-order, and reaction–diffusion models to investigate tumor–immune interactions, spatial heterogeneity, and spatiotemporal dynamics in biological systems [8–10]. Among these variables, age has been widely used in structured cell population models because almost all populations with life cycles can be described using age-structured formulations.

The age-structured cell population models were introduced by Webb [11], which consider the property of asynchronous exponential growth of age-structured cell populations. On the basis of [11], Dyson [12] introduced a proliferating cell population model. The model distinguishes individual cells by their proliferating or quiescent status and allows cells to transit between these two states at any age. Furthermore, based on [12], Liu et al. [13] introduced a variable to consider the impact of nutrients on cell transformation; the model is given as follows:

$$
\begin{cases}
\dfrac{\partial P(t,a)}{\partial t} + k\dfrac{\partial P(t,a)}{\partial a} = -\mu_1(a)P(t,a) - \dfrac{\eta s\beta(a)N(t)P(t,a)}{H+N(t)}, \\
\dfrac{\partial Q(t,a)}{\partial t} + k\dfrac{\partial Q(t,a)}{\partial a} = -\mu_2(a)Q(t,a), \\
\dfrac{\mathrm{d}N(t)}{\mathrm{d}t} = b(\sigma - N(t)) - \dfrac{sN(t)}{H+N(t)}\displaystyle\int_0^\infty P(t,a) + \gamma Q(t,a)\,\mathrm{d}a, \\
P(t,0) = \dfrac{2(1-f)\eta sN(t)}{H+N(t)}\displaystyle\int_0^\infty \beta(a)P(t,a)\,\mathrm{d}a, \\
Q(t,0) = \dfrac{2f\eta sN(t)}{H+N(t)}\displaystyle\int_0^\infty \beta(a)P(t,a)\,\mathrm{d}a, \\
P(0,a) = P_0(a), \quad Q(0,a) = Q_0(a), \quad N(0) = N_0,
\end{cases}
\tag{1.1}
$$

where $P(t,a)$ and $Q(t,a)$ represent the densities of proliferating and quiescent cells, respectively, $N(t)$ represents the concentration of nutrition for $t \in [0,T]$, $T < \infty$ and $a \in [0,\infty)$. The biological interpretation of all model parameters is given in Table 1.

Table 1. Biological explanations for parameters in system (1.1).

Parameters	Description
k	Evolution speed of physiological age with time
$\mu_1(a)$	Death rate of tumor cells in the proliferating stages
$\mu_2(a)$	Death rate of tumor cells in the quiescent stages
η	The conversion factor between nutrient and tumor population
s	The maximal consumption rate of nutrients
H	The subsaturation rate of nutrients
b	The washout rate of nutrients
$b\sigma$	The recruitment rate of nutrients
γ	The ratio of nutrient consumption between proliferating and quiescent cells
f	The fraction of newborn cells that will switch to quiescent with age 0 once they are divided
$\beta(a)$	The division rate related to the age of the proliferating cell

Following the biological interpretation of the original model in [13], the cell age a is measured from the time when a daughter cell is generated by mitosis. Therefore, $P(t,0)$ and $Q(t,0)$ represent the densities of newly generated proliferating and quiescent tumor cells of age zero at time t, respectively. The nonlocal term $\int_0^\infty \beta(a)P(t,a)\,\mathrm{d}a$ represents the age-aggregated division activity of the proliferating cell population, where $\beta(a)$ is the age-dependent division rate. The factor $\dfrac{\eta s N(t)}{H+N(t)}$ describes the nutrient-dependent modulation of cell division. Each dividing proliferating cell produces two daughter cells, of which the fraction $1-f$ enters the proliferating compartment, and the fraction f enters the quiescent compartment. Hence, the two boundary conditions describe the recruitment of newborn proliferating and quiescent cells generated by mitosis across all physiological ages.

In this paper, we make the same assumptions as [14] for system (1.1): none of the proliferating cells with age $a > 0$ will enter the quiescent stage, and $\beta(a) = 0$ for $a > a_\dagger$, where $a_\dagger$ denotes the maximum survival age of a cell. Consequently, all age integrals can be restricted to $[0, a_\dagger]$. Mathematically, it is always assumed that

$$P_0, Q_0 \in L^1_+[0, a_\dagger], \qquad N_0 \geq 0,$$

where $L^1_+[0, a_\dagger] = \left\{u : \int_0^{a_\dagger} |u(a)|\, \mathrm{d}a < \infty, u(a) \geq 0 \text{ for a.e. } a \in [0, a_\dagger]\right\}$, and

$$\begin{aligned} &\beta \in L^\infty_+(0,\infty), 0 \leq \beta(a) \leq \beta_+, \\ &\mu_i \in L^\infty_+(0,\infty), 0 < \mu_- \leq \mu_i(a) \leq \mu_+, \quad i = 1, 2, \end{aligned} \tag{1.2}$$

where $L^\infty_+(0,\infty) = \left\{u : \sup\limits_{a\in(0,\infty)} |u(a)| < \infty\right\}$. Additionally, the functions β and μ_i are Lipschitz continuous.

Many scholars have proposed a series of numerical methods for cell population models without age. In [15], authors considered multi-variable cell population balance models using several different numerical methods; it was shown that time-explicit methods are, in general, far more efficient than time-implicit methods. Among the time-explicit methods, compared to multi-step methods, the higher time accuracy of one-step Runge-Kutta methods can result in higher stability limits. [16] considered the finite element approximation to the generalized multi-variable cell population balance problem and indicated that finite element methods were far worse than the best spectral and finite difference methods for the multi-variable cell population balance model. In [17], authors used numerical methods to study in vitro human tumor cell population models and found that the pseudo-spectral method requires a much smaller number of grid points than those needed for the finite difference method to reach comparable accuracy. Moreover, there are also many high-order numerical methods, such as the second-order approximation of the exact solution of a SIPCV epidemic model obtained through the trapezoidal formula in [18]. However, numerical methods of age-structured cell population models are rarely studied.

Compared to the numerical methods mentioned above, the continuous collocation method [19] demonstrates superior applicability for age-structured tumor cell population models. In fact, the accuracy of finite difference methods is relatively limited. Finite element methods can be complex in dealing with integral and coupled terms. Spectral methods [20, 21] require higher smoothness and may produce negative solutions (see Example 7.4 in Section 7). However, the continuous collocation methods ensure both the accuracy and nonnegativity of numerical solutions, which satisfies the biological significance of the models.

Due to the existence and importance of the evolution speed k in system (1.1), it will result in a strong dependence on the parameter k if we discrete the system directly. Therefore, we consider the semi-discrete method to avoid this dependence. Unlike the characteristic line method in [22], which requires the age step size and time step size to be consistent, we propose an abstract age-semi-discrete scheme through the r-stage continuous collocation method.

For age-structured models, high-order approximation of the basic reproduction number R_0 is more essential than convergence analysis of numerical solutions, as R_0 is a key threshold of the stability and is generally hard to evaluate exactly. In this paper, the numerical basic reproduction number R_h is introduced using the r-stage collocation method. Some conditions are provided such that R_h is at least an $r+1$ order approximation of R_0, and R_h is a threshold of the age-semi-discrete scheme.

Building on the semi-discrete framework, we proceed to the time-full discretization. A key challenge is that the nonlinear coupling, together with age discretization, produces large, dense matrices that render fully implicit methods computationally prohibitive. To address this, we introduce a linearly implicit Euler method that treats the birth terms explicitly and the remaining terms implicitly. This approach preserves the order of accuracy of the collocation scheme and retains the stability threshold R_h established in the semi-discrete analysis.

The organization of this paper is as follows: The continuous collocation methods are reviewed, and the age-semi-discrete scheme is presented in Section 2. In Section 3, the age-semi-discrete scheme is linearized, and the characteristic equation is obtained. The convergence of R_h and R_0 is studied in Section 4. The stability of the age-semi-discrete system is investigated in Section 5. A time-full-discrete scheme is introduced, and the stability of the time-full-discrete system is given in Section 6. Some numerical experiments illustrate the convergence and stability in Section 7.

2. Age-semi-discrete scheme

2.1. Abstract form of continuous model

In this subsection, we obtain the abstract form and the basic reproduction number R_0 of model (1.1). We denote the spaces by

$$L^1[0,a_\dagger] = \left\{ u : \int_0^{a_\dagger} |u(a)| \,\mathrm{d}a < \infty \right\},$$

and

$$W^{1,1}[0,a_\dagger] = \left\{ u \in L^1[0,a_\dagger] : \frac{\mathrm{d}u}{\mathrm{d}a} \in L^1[0,a_\dagger] \right\},$$

where $\mathrm{d}u/\mathrm{d}a$ denotes the first weak derivative of u with respect to the age variable a.

Set $X = L^1[0,a_\dagger] \times L^1[0,a_\dagger] \times \mathbb{R}$ and define the linear operator $\mathcal{L} : D(\mathcal{L}) \to X$ by

$$\mathcal{L}\begin{pmatrix} \varphi \\ \omega \\ \chi \end{pmatrix} = \begin{pmatrix} -k\varphi' - \mu_1(a)\varphi \\ -k\omega' - \mu_2(a)\omega \\ -b\chi \end{pmatrix},$$

where

$$D(\mathcal{L}) = \left\{ \begin{pmatrix} \varphi \\ \omega \\ \chi \end{pmatrix} \in W^{1,1}[0,a_\dagger] \times W^{1,1}[0,a_\dagger] \times \mathbb{R} : \begin{array}{l} \varphi(0) = \dfrac{2(1-f)\eta s\chi}{H+\chi} \displaystyle\int_0^{a_\dagger} \beta(a)\varphi(a)\,\mathrm{d}a \\ \omega(0) = \dfrac{2f\eta s\chi}{H+\chi} \displaystyle\int_0^{a_\dagger} \beta(a)\varphi(a)\,\mathrm{d}a \end{array} \right\}.$$

Introduce the nonlinear operator $\mathcal{N} : X \to X$ by

$$\mathcal{N}\left(\begin{pmatrix} \varphi \\ \omega \\ \chi \end{pmatrix}\right) = \begin{pmatrix} -\dfrac{\eta s\beta(a)\chi\varphi}{H+\chi} \\ 0 \\ b\sigma - \dfrac{s\chi}{H+\chi}\int_0^{a_\dagger} \varphi(a) + \gamma\omega(a)\,\mathrm{d}a \end{pmatrix}.$$

By setting $U = \begin{pmatrix} \varphi, \omega, \chi \end{pmatrix}^T$, then the abstract form of (1.1) is rewritten as

$$\begin{cases} \dfrac{\mathrm{d}U(t)}{\mathrm{d}t} = \mathcal{L}U(t) + \mathcal{N}(U(t)), \quad t > 0, U(t) \in D(\mathcal{L}), \\ U(0) = U_0, \end{cases} \tag{2.1}$$

where $U_0 = \begin{pmatrix} P_0(a), Q_0(a), N_0 \end{pmatrix}^T$.

From [13], linearizing the system (1.1) at steady state $(0, 0, \sigma)^T$, we introduce the linear operator $\hat{\mathcal{L}} : D(\hat{\mathcal{L}}) \to X$ by

$$\hat{\mathcal{L}}\begin{pmatrix} \hat{\varphi} \\ \hat{\omega} \\ \hat{\chi} \end{pmatrix} = \begin{pmatrix} -k\hat{\varphi}' - \mu_1(a)\hat{\varphi} - \dfrac{\eta s\beta(a)\sigma}{H+\sigma}\hat{\varphi} \\ -k\hat{\omega}' - \mu_2(a)\hat{\omega} \\ -b\hat{\chi} - \dfrac{s\sigma}{H+\sigma}\int_0^{a_\dagger} \hat{\varphi}(a) + \gamma\hat{\omega}(a)\,\mathrm{d}a \end{pmatrix},$$

where

$$D(\hat{\mathcal{L}}) = \left\{ \begin{pmatrix} \hat{\varphi} \\ \hat{\omega} \\ \hat{\chi} \end{pmatrix} \in W^{1,1}[0, a_\dagger] \times W^{1,1}[0, a_\dagger] \times \mathbb{R} : \begin{matrix} \hat{\varphi}(0) = \dfrac{2(1-f)\eta s\sigma}{H+\sigma}\displaystyle\int_0^{a_\dagger} \beta(a)\hat{\varphi}(a)\,\mathrm{d}a \\ \hat{\omega}(0) = \dfrac{2f\eta s\sigma}{H+\sigma}\displaystyle\int_0^{a_\dagger} \beta(a)\hat{\varphi}(a)\,\mathrm{d}a \end{matrix} \right\}.$$

By setting $X = \begin{pmatrix} \hat{\varphi}, \hat{\omega}, \hat{\chi} \end{pmatrix}^T$, then the abstract form after linearization of (1.1) is rewritten as

$$\begin{cases} \dfrac{\mathrm{d}X(t)}{\mathrm{d}t} = \hat{\mathcal{L}}X(t), \quad t > 0, \quad X(t) \in D(\hat{\mathcal{L}}), \\ X(0) = U_0. \end{cases} \tag{2.2}$$

Apart from the always stable eigenvalue $\lambda = -b$, the remaining eigenvalues satisfy

$$d(\lambda) = 1 - \frac{2(1-f)\eta s\sigma}{H+\sigma}\int_0^{a_\dagger} \beta(a)\hat{\varphi}(a,\lambda)\,\mathrm{d}a = 0,$$

where $\hat{\varphi}(a, \lambda)$ is a solution to

$$\begin{cases} k\hat{\varphi}' = -\mu_1(a)\hat{\varphi} - \dfrac{\eta s\beta(a)\sigma}{H+\sigma}\hat{\varphi} - \lambda\hat{\varphi}. \\ \hat{\varphi}(0) = 1. \end{cases} \tag{2.3}$$

The basic reproduction number is also provided by

$$R_0 = \frac{2(1-f)\eta s\sigma}{H+\sigma}\int_0^{a_\dagger} \beta(a)\hat{\varphi}(a,0)\,\mathrm{d}a, \tag{2.4}$$

where $\hat{\varphi}(a, 0)$ is defined by (2.3).

2.2. Continuous collocation methods

In this subsection, we review the definition and other conclusions of collocation methods for ordinary differential equations in [23].

Consider the initial-value problem

$$\begin{aligned} y' &= f(a, y), \quad a \in [a_0, a_1] \\ y(a_0) &= y_0. \end{aligned} \tag{2.5}$$

Definition 2.1. *Let $c_1, \cdots, c_r$ be distinct real numbers (usually $0 \le c_i \le 1$). The collocation polynomial $g(a)$ is a polynomial of degree r satisfying*

$$\begin{aligned} g'(a_0 + c_i h) &= f(a_0 + c_i h, g(a_0 + c_i h)), \quad i = 1, \ldots, r, \\ g(a_0) &= g_0 \end{aligned}$$

and the numerical solution of the collocation method is defined by $y_1 = g(a_0 + h)$.

Lemma 2.1. *[23] The collocation method of Definition 2.1 is equivalent to the r-stage Runge-Kutta method with coefficients*

$$a_{ij} = \int_0^{c_i} \ell_j(\tau) d\tau, \quad b_i = \int_0^1 \ell_i(\tau) d\tau, \tag{2.6}$$

where $\ell_i(\tau) = \prod\limits_{l \neq i} \dfrac{(\tau - c_l)}{(c_i - c_l)}, i = 1, \cdots, r$ is the Lagrange polynomial.

Since $\tau^{k-1} = \sum\limits_{j=1}^{r} c_j^{k-1} \ell_j(\tau)$, $k = 1, \ldots, m$, the relations (2.6) are equivalent to the linear systems

$$\begin{aligned} C(p): \quad & \sum_{j=1}^{r} a_{ij} c_j^{k-1} = \frac{c_i^k}{k}, \quad k = 1, \ldots, p, \text{ all } i, \\ B(s): \quad & \sum_{i=1}^{r} b_i c_i^{k-1} = \frac{1}{k}, \quad k = 1, \ldots, s, \end{aligned}$$

with $p = r$ and $s = r$.

Lemma 2.2. *[23] If the condition $B(s)$ holds for some $s \ge r$, then the continuous collocation methods have order p. This means that the continuous collocation methods have the same order as the underlying quadrature formula.*

Lemma 2.3. *[23] The collocation polynomial $g(t)$ is an approximation of order m to the exact solution of (2.5) on the whole interval, that is,*

$$\|g(a) - y(a)\| \le C h^{r+1}, \quad \textit{for } a \in [a_0, a_0 + h]$$

and for sufficiently small h.

2.3. Age-semi-discrete scheme

In this subsection, we consider an age-semi-discrete method for the model (1.1). Let N, which is greater than 0 and independent of k, be an integer and $\{a_0 = 0 < a_1 < \cdots < a_n < \cdots < a_N = a_\dagger\}$ be the age mesh. Different from the characteristic line methods, the age-semi-discretization can be established under a general age mesh. However, for convenience, we will discuss the age-semi-discretization under a uniform mesh as $a_n = nh, n = 0, 1, \cdots, N$ with $h = \dfrac{a_\dagger}{N}$.

Denote the numerical space by

$$\mathcal{Y}_h = \left\{ \begin{pmatrix} \varphi_h \\ \omega_h \end{pmatrix} \in C[0, a_\dagger] \times C[0, a_\dagger] : \varphi_h \Big|_{[a_n, a_{n+1}]} \in \Pi_r, \omega_h \Big|_{[a_n, a_{n+1}]} \in \Pi_r \right\},$$

with $n = 0, 1, \cdots, N-1$, of which the dimension is $2(rN + 1)$, and Π_r is the space of polynomials with degree less than or equal to r. For given collocation parameters $0 < c_1 < \cdots < c_r \leq 1$, let

$$\mathcal{M}_h = \{a_i^n \mid a_i^n = a_n + c_i h, n = 0, 1, \cdots, N-1, i = 1, 2, \cdots, r\}$$

be the collocation mesh points and $X_h = \mathcal{Y}_h \times \mathbb{R}$.

Define the numerical linear operator $\mathcal{L}_h : D(\mathcal{L}_h) \to X_h$ by

$$\mathcal{L}_h \begin{pmatrix} \varphi_h \\ \omega_h \\ \chi_h \end{pmatrix} = \begin{pmatrix} -k\varphi_h' - \mu_1(a)\varphi_h \\ -k\omega_h' - \mu_2(a)\omega_h \\ -b\chi_h \end{pmatrix}, \quad \text{for } a \in \mathcal{M}_h,$$

where

$$D(\mathcal{L}_h) = \left\{ \begin{pmatrix} \varphi_h \\ \omega_h \\ \chi_h \end{pmatrix} \in X_h : \begin{array}{l} \varphi_h(0) = \dfrac{2(1-f)\eta s \chi_h}{H + \chi_h} \displaystyle\sum_{n=0}^{N-1} h \sum_{i=1}^{r} b_i \beta_i^n \varphi_{hi}^n \\ \omega_h(0) = \dfrac{2f\eta s \chi_h}{H + \chi_h} \displaystyle\sum_{n=0}^{N-1} h \sum_{i=1}^{r} b_i \beta_i^n \varphi_{hi}^n \end{array} \right\}.$$

Then, introduce the nonlinear operator $\mathcal{N}_h : X_h \to X_h$ by

$$\mathcal{N}_h \left(\begin{pmatrix} \varphi_h \\ \omega_h \\ \chi_h \end{pmatrix} \right) = \begin{pmatrix} -\dfrac{\eta s \beta(a) \chi_h \varphi_h}{H + \chi_h} \\ 0 \\ b\sigma - \dfrac{s\chi_h}{H + \chi_h} \sum\limits_{n=0}^{N-1} h \sum\limits_{i=1}^{r} b_i (\varphi_{hi}^n + \gamma \omega_{hi}^n) \end{pmatrix},$$

where $\beta_i^n = \beta\left(a_i^n\right), \varphi_{hi}^n = \varphi_h\left(a_i^n\right), \omega_{hi}^n = \omega_h\left(a_i^n\right)$ for $n = 0, \ldots, N-1$ and $i = 1, \ldots, r$, and we also define two projection operators $\hat{\mathcal{P}}_h : W^{1,1}[0, a_\dagger] \times W^{1,1}[0, a_\dagger] \to \mathcal{Y}_h$ and $\mathcal{P}_h : X \to D(\mathcal{L}_h)$ by

$$\hat{\mathcal{P}}_h \begin{pmatrix} \varphi \\ \omega \end{pmatrix} = \begin{pmatrix} \varphi \\ \omega \end{pmatrix}, \quad \text{for } a \in \mathcal{M}_h \cup \{a_0\},$$

and

$$\mathcal{P}_h \begin{pmatrix} \varphi \\ \omega \\ \chi \end{pmatrix} = \begin{pmatrix} \hat{\mathcal{P}}_h \begin{pmatrix} \varphi \\ \omega \end{pmatrix} \\ \chi \end{pmatrix}, \quad \text{for } a \in \mathcal{M}_h \cup \{a_0\}.$$

Then an age-semi-discrete solution is defined as follows.

Definition 2.2. *A differentiable function $U_h(t)$, a mapping from $[0,\infty) \to D(\mathcal{L}_h)$, is called an age-semi-discrete solution of (2.1) if it satisfies the semi-discrete system*

$$\begin{cases} \dfrac{\mathrm{d}U_h(t)}{\mathrm{d}t} = \mathcal{L}_h U_h(t) + \mathcal{N}_h(U_h(t)), \quad a \in \mathcal{M}_h, \\ U_h(0) = \mathcal{P}_h U_0. \end{cases} \tag{2.7}$$

Remark 2.1. $(0,0,\sigma)^T \in X_h$ *is also an equilibrium of* (2.7).

3. Linearization and characteristic equation

In this section, we linearize system (2.7) at $(0,0,\sigma)^T$. According to $X_h = \mathcal{Y}_h \times \mathbb{R}$, define the numerical linear operator $\hat{\mathcal{L}}_h : D(\hat{\mathcal{L}}_h) \to X_h$ by

$$\hat{\mathcal{L}}_h \begin{pmatrix} \hat{\varphi}_h \\ \hat{\omega}_h \\ \hat{\chi}_h \end{pmatrix} = \begin{pmatrix} -k\hat{\varphi}_h' - \mu_1(a)\hat{\varphi}_h - \dfrac{\eta s \beta(a)\sigma}{H+\sigma}\hat{\varphi}_h \\ -k\hat{\omega}_h' - \mu_2(a)\hat{\omega}_h \\ -b\hat{\chi}_h - \dfrac{s\sigma}{H+\sigma}\sum_{n=0}^{N-1} h \sum_{i=1}^{r} b_i(\hat{\varphi}_{hi}^n + \gamma\hat{\omega}_{hi}^n) \end{pmatrix}, \; a \in \mathcal{M}_h,$$

where

$$D(\hat{\mathcal{L}}_h) = \left\{ \begin{pmatrix} \hat{\varphi}_h \\ \hat{\omega}_h \\ \hat{\chi}_h \end{pmatrix} \in X_h : \begin{array}{l} \hat{\varphi}_h(0) = \dfrac{2(1-f)\eta s\sigma}{H+\sigma} \displaystyle\sum_{n=0}^{N-1} h \sum_{i=1}^{r} b_i\beta_i^n \hat{\varphi}_{hi}^n \\ \hat{\omega}_h(0) = \dfrac{2f\eta s\sigma}{H+\sigma} \displaystyle\sum_{n=0}^{N-1} h \sum_{i=1}^{r} b_i\beta_i^n \hat{\varphi}_{hi}^n \end{array} \right\}.$$

Definition 3.1. *A differentiable function $X_h(t)$, a mapping from $[0,\infty) \to D(\hat{\mathcal{L}}_h)$, is called an age-semi-discrete solution of (2.2) if it satisfies the semi-discrete system*

$$\begin{cases} \dfrac{\mathrm{d}X_h(t)}{\mathrm{d}t} = \hat{\mathcal{L}}_h X_h(t), \quad X_h(t) \in D(\hat{\mathcal{L}}_h), \quad a \in \mathcal{M}_h, \\ X(0) = \mathcal{P}_h U_0. \end{cases} \tag{3.1}$$

Consider the characteristic equation of system (3.1),

$$\lambda_h \begin{pmatrix} \hat{\varphi}_h \\ \hat{\omega}_h \\ \hat{\chi}_h \end{pmatrix} = \hat{\mathcal{L}}_h \begin{pmatrix} \hat{\varphi}_h \\ \hat{\omega}_h \\ \hat{\chi}_h \end{pmatrix}, \quad \begin{pmatrix} \hat{\varphi}_h \\ \hat{\omega}_h \\ \hat{\chi}_h \end{pmatrix} \in D(\hat{\mathcal{L}}_h),$$

that is,

$$\begin{cases} \lambda_h\hat{\varphi}_h = -k\hat{\varphi}_h' - \mu_1(a)\hat{\varphi}_h - \dfrac{\eta s\beta(a)\sigma}{H+\sigma}\hat{\varphi}_h, \quad a \in \mathcal{M}_h, \\ \lambda_h\hat{\omega}_h = -k\hat{\omega}_h' - \mu_2(a)\hat{\omega}_h, \quad a \in \mathcal{M}_h, \\ \lambda_h\hat{\chi}_h = -b\hat{\chi}_h - \dfrac{s\sigma}{H+\sigma}\sum_{n=0}^{N-1} h \sum_{i=1}^{r} b_i\left(\hat{\varphi}_h(a_i^n,\lambda_h) + \gamma\hat{\omega}_h(a_i^n,\lambda_h)\right), \\ \hat{\varphi}_h(0) = \dfrac{2(1-f)\eta s\sigma}{H+\sigma}\sum_{n=0}^{N-1} h \sum_{i=1}^{r} b_i\beta_i^n\hat{\varphi}_h(a_i^n,\lambda_h), \\ \hat{\omega}_h(0) = \dfrac{2f\eta s\sigma}{H+\sigma}\sum_{n=0}^{N-1} h \sum_{i=1}^{r} b_i\beta_i^n\hat{\varphi}_h(a_i^n,\lambda_h). \end{cases} \tag{3.2}$$

Here, $\hat{\chi}_h \in \mathbb{R}$ is independent of the age variable a. Therefore, no boundary condition at $a = 0$ is required for $\hat{\chi}_h$.

For the first equation of (3.2), let $\hat{\varphi}_h(0) = 1$, then $\hat{\varphi}_h(a_i^n, \lambda_h)$ satisfies

$$\begin{cases} \lambda_h \hat{\varphi}_h = -k\hat{\varphi}_h' - \mu_1(a)\hat{\varphi}_h - \dfrac{\eta s \beta(a)\sigma}{H+\sigma}\hat{\varphi}_h, \quad a \in \mathcal{M}_h, \\ \hat{\varphi}_h(0) = 1, \end{cases} \tag{3.3}$$

therefore, $\hat{\varphi}_h(a_i^n, \lambda_h) \in \mathcal{Y}_h$ is a collocation solution to

$$\begin{cases} k\hat{\varphi}' = -\mu_1(a)\hat{\varphi} - \dfrac{\eta s \beta(a)\sigma}{H+\sigma}\hat{\varphi} - \lambda_h \hat{\varphi}, \quad a \in [0, a_\dagger], \\ \hat{\varphi}(0) = 1. \end{cases}$$

Similarly, for the second equation of (3.2), $\hat{\omega}_h(a_i^n, \lambda_h)$ is a collocation solution to

$$\begin{cases} k\hat{\omega}' = -\mu_2(a)\hat{\omega} - \lambda_h \hat{\omega}, \quad a \in [0, a_\dagger], \\ \hat{\omega}(0) = 1. \end{cases}$$

Then the matrix representation of (3.2) is as follows:

$$\begin{pmatrix} 1 - \dfrac{2(1-f)\eta s\sigma}{H+\sigma} \sum\limits_{n=0}^{N-1} h \sum\limits_{i=1}^{r} b_i \beta_i^n \hat{\varphi}_h(a_i^n, \lambda_h) & 0 & 0 \\ -\dfrac{2f\eta s\sigma}{H+\sigma} \sum\limits_{n=0}^{N-1} h \sum\limits_{i=1}^{r} b_i \beta_i^n \hat{\varphi}_h(a_i^n, \lambda_h) & 1 & 0 \\ \dfrac{s\sigma}{H+\sigma} \sum\limits_{n=0}^{N-1} h \sum\limits_{i=1}^{r} b_i \hat{\varphi}_h(a_i^n, \lambda_h) & \dfrac{s\gamma\sigma}{H+\sigma} \sum\limits_{n=0}^{N-1} h \sum\limits_{i=1}^{r} b_i \hat{\omega}_h(a_i^n, \lambda_h) & \lambda_h + b \end{pmatrix} \begin{pmatrix} \hat{\varphi}_h(0) \\ \hat{\omega}_h(0) \\ \hat{\chi}_h \end{pmatrix} = 0. \tag{3.4}$$

Denote (3.4) as $G(\lambda_h)\begin{pmatrix} \hat{\varphi}_h(0) \\ \hat{\omega}_h(0) \\ \hat{\chi}_h \end{pmatrix} = 0$, which yields $\det(G(\lambda_h)) = 0$, then the eigenvalues consist of the always stable eigenvalue $\lambda_h = -b$ and the roots of

$$d_h(\lambda_h) = 1 - \frac{2(1-f)\eta s\sigma}{H+\sigma} \sum_{n=0}^{N-1} h \sum_{i=1}^{r} b_i \beta_i^n \hat{\varphi}_h(a_i^n, \lambda_h) = 0.$$

Therefore, the stability is determined by the roots of $d_h(\lambda_h) = 0$.

Following the methodology established in [13] for defining the analytical basic reproduction number R_0 through the characteristic equation approach, we can derive the numerical basic reproduction number R_h for the age-semi-discrete system (2.7).

Definition 3.2. *A numerical basic reproduction number R_h for the age-semi-discrete system* (2.7) *is defined by*

$$R_h = \frac{2(1-f)\eta s\sigma}{H+\sigma} \sum_{n=0}^{N-1} h \sum_{i=1}^{r} b_i \beta_i^n \hat{\varphi}_h(a_i^n, 0), \tag{3.5}$$

where $\hat{\varphi}_h(a_i^n, 0)$ is defined by (3.3).

From (2.4) and (3.5), we can see that the numerical basic reproduction number is similar to the exact basic reproduction number, but it is not directly defined by quadrature to the exact basic reproduction number. In the next section, we will show that R_h is a higher-order approximation to R_0 with at least $r+1$ order.

4. Convergence

In this section, we will discuss the higher-order convergence between R_0 and R_h with the assumption (1.2). The error of the numerical basic reproduction number is expressed as follows:

$$|R_h - R_0| = \frac{2(1-f)\eta s\sigma}{H+\sigma}\left|\sum_{n=0}^{N-1} h\sum_{i=1}^{r} b_i\beta_i^n\hat{\varphi}_{hi}^n - \int_0^{a_\dagger}\beta(a)\hat{\varphi}(a)\,\mathrm{d}a\right|.$$

Next, we can convert the error into the following two parts:

$$\begin{aligned}
&\frac{2(1-f)\eta s\sigma}{H+\sigma}\left|\sum_{n=0}^{N-1} h\sum_{i=1}^{r} b_i\beta_i^n\hat{\varphi}_{hi}^n - \int_0^{a_\dagger}\beta(a)\hat{\varphi}(a)\,\mathrm{d}a\right| \\
\leq\ & \frac{2(1-f)\eta s\sigma}{H+\sigma}\left(\sum_{n=0}^{N-1}\left|h\sum_{i=1}^{r} b_i\beta_i^n\hat{\varphi}_{hi}^n - \int_{a_n}^{a_{n+1}}\beta(a)\hat{\varphi}_h(a)\,\mathrm{d}a\right| + \sum_{n=0}^{N-1}\left|\int_{a_n}^{a_{n+1}}\beta(a)(\hat{\varphi}_h(a)-\hat{\varphi}(a))\,\mathrm{d}a\right|\right) \\
=\ & \frac{2(1-f)\eta s\sigma}{H+\sigma}\left(I_1+I_2\right),
\end{aligned}$$

where

$$I_1 = \sum_{n=0}^{N-1}\left|h\sum_{i=1}^{r} b_i\beta_i^n\hat{\varphi}_{hi}^n - \int_{a_n}^{a_{n+1}}\beta(a)\hat{\varphi}_h(a)\,\mathrm{d}a\right|$$

is called the quadrature error, and

$$I_2 = \sum_{n=0}^{N-1}\left|\int_{a_n}^{a_{n+1}}\beta(a)(\hat{\varphi}_h(a)-\hat{\varphi}(a))\,\mathrm{d}a\right|$$

is called the collocation error.

Then we just need to consider the errors of I_1 and I_2. For the superconvergence analysis, we further assume that

$$\beta, \mu_1 \in C^{r+\kappa}[0, a_\dagger].$$

Theorem 4.1. *Assume that $\beta \in C^{r+\kappa}[0, a_\dagger]$, $\mu_1 \in C^{r+\kappa}[0, a_\dagger]$. If the r collocation parameters $\{c_i\}$ are subject to the orthogonality condition*

$$J_v = \int_0^1 s^v \prod_{i=1}^{r}(s-c_i)\,\mathrm{d}s = 0,$$

for $v = 0, 1, \cdots, \kappa-1$, and $\kappa = 1, 2, \cdots, r$, then the quadrature error

$$I_1 \leq C_1 h^{r+\kappa},$$

and the collocation error

$$I_2 \le C_2 h^{r+\kappa},$$

where C_1 and C_2 are independent of h but depend on $\{c_i\}$.

Proof. The proof is given in Appendix A.1. □

Remark 4.1. *For the Gauss collocation method, the orthogonality index satisfies $\kappa = r$, and hence, the convergence order is $2r$. For the Radau IIA collocation method, $\kappa = r - 1$, which gives the convergence order $2r - 1$. These theoretical orders are confirmed by the numerical results reported in Table 2.*

The above convergence result shows that R_h provides a high-order approximation to R_0. However, convergence alone does not guarantee that the discrete system preserves the threshold dynamics of the continuous model. Therefore, in the next section, we investigate whether R_h also determines the local stability of the age-semi-discrete system.

5. Stability

In this section, we will discuss the stability condition of the solution of the age-semi-discrete system (2.7) and obtain that the numerical basic reproduction number R_h is the threshold for the age-semi-discrete system. We do some preparations before stating the stability.

Lemma 5.1. *[24] For $\lambda \in \mathbb{C}$, the collocation solution $\hat{\varphi}_h$ is an approximation of order r to the exact solution $\hat{\varphi}$ on the whole interval, that is,*

$$\left\| \hat{\varphi}_h(a_i^n, \lambda) - \hat{\varphi}(a, \lambda) \right\| \le C_0 h^r, \quad \text{for } a \in [0, a_\dagger],$$

where $C_0 = C_0(\lambda)$.

According to Lemma 5.1, the following lemma is trivial.

Lemma 5.2. *[24] For each fixed $\lambda \in \mathbb{C}$, let $d(\lambda)$ and $d_h(\lambda)$ denote the continuous and discrete characteristic functions, respectively, defined by*

$$d(\lambda) = 1 - \frac{2(1-f)\eta s\sigma}{H+\sigma} \int_0^{a_\dagger} \beta(a)\hat{\varphi}(a, \lambda)\, \mathrm{d}a,$$

and

$$d_h(\lambda) = 1 - \frac{2(1-f)\eta s\sigma}{H+\sigma} \sum_{n=0}^{N-1} h \sum_{i=1}^{r} b_i \beta(a_i^n)\hat{\varphi}_h(a_i^n, \lambda).$$

Then, we have

$$|d_h(\lambda) - d(\lambda)| \le C_1 h^r,$$

where $C_1 = C_1(\lambda)$.

Lemma 5.3. *[24] If the function $d(\lambda)$ has a zero $\bar{\lambda} \in \mathbb{C}$ with multiplicity v, which is $d(\bar{\lambda}) = 0, \cdots,$ $d^{(v-1)}(\bar{\lambda}) = 0$, $d^{(v)}(\bar{\lambda}) \neq 0$, then there exists a $\gamma_0 > 0$ such that for $\lambda \in B(\bar{\lambda}, \gamma_0) \backslash \left\{\bar{\lambda}\right\}$*

$$|d(\lambda)| > C_2 \left\| \lambda - \bar{\lambda} \right\|^v,$$

where $C_2 = C_2(\bar{\lambda}, \gamma_0)$.

According to the above lemmas, we can obtain the relationship between the zeros of $d(\lambda)$ and $d_h(\lambda)$.

Theorem 5.1. *If the function $d(\lambda)$ has a zero $\bar{\lambda} \in \mathbb{C}$ with multiplicity v and $h \le \left(\frac{C_2\gamma_0^v}{C_1}\right)^{\frac{1}{r}}$, then $d_h(\lambda)$ has v zeros $\lambda_h \in B(\bar{\lambda}, \gamma_0)$, $h = 1, 2, \cdots, v$ (taking multiplicities into account); moreover,*

$$\max_{1\le h\le v} \left|\bar{\lambda} - \lambda_h\right| \le \left(\frac{C_1 h^r}{C_2}\right)^{\frac{1}{v}},$$

where C_1 is mentioned in Lemma 5.2, and C_2 and γ_0 are mentioned in Lemma 5.3.

Proof. The proof is given in Appendix A.2. □

The study of the stability condition for the age-semi-discrete system is based on the consideration that β is a constant function, and it can be concluded that R_h is also a threshold for the age-semi-discrete system.

Theorem 5.2. *Assume that $\beta(a) = \beta^*$, where β^* is a positive constant. When the coefficients of the Runge-Kutta method satisfy*

(i) $b_i \ge 0$, *for* $i = 1, 2, \cdots, r$,

(ii) $M = \left(m_{ij}\right) = \left(b_i a_{ij} + b_j a_{ji} - b_i b_j\right)_{i,j=1}^r$ *is nonnegative definite,*

and the step size h is sufficiently small, the numerical basic reproduction number R_h is the threshold for the age-semi-discrete system, i.e., the numerical age-semi-discrete solution $U_h(t)$ is asymptotically stable if and only if $R_h < 1$.

Proof. The proof is given in Appendix A.3. □

Remark 5.1. *The Runge-Kutta method, which satisfies (i) and (ii) in Theorem 5.2 (see [25]), is called algebraically stable. Since both the Gauss and Radau IIA collocation methods are algebraically stable, they are employed in the subsequent numerical experiments to verify the stability of the proposed numerical scheme.*

Remark 5.2. *In Theorem 5.2, we only consider constant $\beta(a) = \beta^*$. We now address the age-dependent case $\beta(a)$ defined on the discrete age mesh $\mathcal{M}_h$. Since the implicit Euler method is a one-stage Runge–Kutta method with $A = (1)$, $B = (1)$, and $c = (1)$, its unique stage point satisfies $a_1^n = a_{n+1}$. Consequently, the stage value coincides with the endpoint value, namely,*

$$\Phi_h(a_1^n, \lambda_h) = \hat{\varphi}_h(a_{n+1}, \lambda_h).$$

Therefore, for $n = 0, \ldots, N-1$, we have

$$\hat{\varphi}_h(a_{n+1}, \lambda_h) = \Phi_h(a_1^n, \lambda_h) = \hat{\varphi}_h(a_n, \lambda_h) - \frac{h}{k}\left(\mu_1(a_{n+1}) + \frac{\eta s\beta(a_{n+1})\sigma}{H+\sigma} + \lambda_h\right)\Phi_h(a_1^n, \lambda_h). \tag{5.1}$$

Then, we obtain

$$\hat{\varphi}_h(a_{n+1}, \lambda_h) = \left[1 + \frac{h}{k}\left(\mu_1(a_{n+1}) + \frac{\eta s\beta(a_{n+1})\sigma}{H+\sigma} + \lambda_h\right)\right]^{-1} \hat{\varphi}_h(a_n, \lambda_h).$$

Since $\hat{\varphi}_h(0) = 1$, as established in the proof of Theorem 5.2, iterating this recurrence relation yields

$$\hat{\varphi}_h(a_{n+1}, \lambda_h) = \hat{\varphi}_h(0) \prod_{m=0}^{n} \left[1 + \frac{h}{k} \left(\mu_1(a_{m+1}) + \frac{\eta s \beta(a_{m+1}) \sigma}{H + \sigma} + \lambda_h \right) \right]^{-1} = \prod_{m=0}^{n} R(z_m), \tag{5.2}$$

where $z_m = -\frac{h}{k}\left(\mu_1(a_{m+1}) + \frac{\eta s \beta\,(a_{m+1})\,\sigma}{H + \sigma} + \lambda_h \right)$, *and* $R(z) = \frac{1}{1-z}$ *is the stability function of the implicit Euler method. It follows from the proof of Theorem 5.2 that*

$$\begin{aligned} S_h &= \frac{2(1-f)\eta s \sigma}{H+\sigma} \sum_{n=0}^{N-1} h \beta(a_{n+1}) \hat{\varphi}_h(a_{n+1}, \lambda_h) \\ &= \frac{2(1-f)\eta s \sigma}{H+\sigma} \sum_{n=0}^{N-1} h \beta(a_{n+1}) \prod_{m=0}^{n} R(z_m) \longrightarrow 0, \qquad \lambda_h \to +\infty. \end{aligned}$$

Therefore, the same stability conclusion as that established in Theorem 5.2 remains valid when β is age-dependent.

Having established the threshold property of R_h for the age-semi-discrete system, we next introduce a time discretization to obtain a fully implementable numerical scheme. The main objective is to determine whether the resulting full-discrete system retains the same stability threshold.

6. Time-full-discrete scheme

6.1. Matrix representation for the age-semi-discrete system

In order to discuss the full discretization, we first consider the matrix representation for the abstract form (2.7). Denote an extension numerical space by

$$\mathcal{Z}_h = \left\{ \begin{pmatrix} P_h \\ Q_h \end{pmatrix} \in L^\infty[0, a_\dagger] \times L^\infty[0, a_\dagger] : P_h \Big|_{[a_n, a_{n+1}]} \in \Pi_r, Q_h\Big|_{[a_n, a_{n+1}]} \in \Pi_r \right\},$$

with $n = 0, 1, \cdots, N-1$.

According to Runge-Kutta methods, for $P_h \in \mathcal{Z}_h$, we have

$$\begin{cases} P_h(a_n + vh) = P_h(a_0^n) + h \sum\limits_{j=1}^{r} \beta_j(v) Y_n^j, \\ Y_n^j = P_h'(a_n + c_j h), \end{cases}$$

where $A = (a_{ij})_{r\times r}$, $a_{ij} = \beta_j(c_i)$, $B = (b_1, b_2, \cdots, b_r)^T$, $b_j = \beta_j(1)$, $i, j = 1, 2, \cdots, r$. Then, we obtain

$$P_h(a_n + c_i h) = P_h(a_0^n) + h \sum_{j=1}^{r} a_{ij} P_h'(a_n + c_j h),$$

that is, for $n = 0, 1, \cdots, N-1$,

$$\begin{pmatrix} P_h'(a_1^n) \\ P_h'(a_2^n) \\ \vdots \\ P_h'(a_r^n) \end{pmatrix} = \frac{1}{h} \begin{pmatrix} a_{11} & a_{12} & \cdots & a_{1r} \\ a_{21} & a_{22} & \cdots & a_{2r} \\ \vdots & \vdots & \vdots & \vdots \\ a_{r1} & a_{r2} & \cdots & a_{rr} \end{pmatrix}^{-1} \begin{pmatrix} -1 & 1 & & \\ -1 & & 1 & \\ \vdots & & & \ddots & \\ -1 & & & & 1 \end{pmatrix} \begin{pmatrix} P_h(a_0^n) \\ P_h(a_1^n) \\ \vdots \\ P_h(a_r^n) \end{pmatrix} = \frac{1}{h} A^{-1} E \begin{pmatrix} P_h(a_0^n) \\ P_h(a_1^n) \\ \vdots \\ P_h(a_r^n) \end{pmatrix},$$

where $E = \begin{pmatrix} -1 & 1 & & & \\ -1 & & 1 & & \\ \vdots & & & \ddots & \\ -1 & & \cdots & & 1 \end{pmatrix} \in \mathbb{R}^{r\times(r+1)}$.

Remark 6.1. *The invertibility of A can be verified according to Theorem 1.1.1 in [26]. In Lemma 2.1, the collocation methods and the Runge-Kutta methods are equivalent, if and only if the relation*

$$\sum_{j=1}^{r} a_{i,j} c_j^{\nu-1} = \frac{c_i^{\nu}}{\nu}, \quad \nu = 1, \ldots, r, \quad i = 1, \ldots, r$$

holds. Then, we can obtain

$$A \begin{pmatrix} c_1^0 & c_1^1 & \cdots & c_1^{r-1} \\ c_2^0 & c_2^1 & \cdots & c_2^{r-1} \\ \vdots & \vdots & & \vdots \\ c_r^0 & c_r^1 & \cdots & c_r^{r-1} \end{pmatrix} = \begin{pmatrix} c_1^1 & c_1^2 & \cdots & c_1^r \\ c_2^1 & c_2^2 & \cdots & c_2^r \\ \vdots & \vdots & & \vdots \\ c_r^1 & c_r^2 & \cdots & c_r^r \end{pmatrix} \begin{pmatrix} 1 & & & \\ & \frac{1}{2} & & \\ & & \ddots & \\ & & & \frac{1}{r} \end{pmatrix}.$$

According to the properties of Vandermonde matrices, A is invertible.

For the matrix representation, for $n = 0, 1, \cdots, N-1$, we define the following matrices: the evolution matrix

$$\mathcal{E}_h^n = \begin{pmatrix} 0 & & & \\ & 1 & & \\ & & \ddots & \\ & & & 1 \end{pmatrix} \in \mathbb{R}^{(r+1)\times(r+1)},$$

the growth matrix

$$\mathcal{A}_h^n = -\frac{k}{h} \begin{pmatrix} \frac{h}{k} & 0 & \cdots & 0 \\ 0 & & & \\ \vdots & & A^{-1} & \\ 0 & & & \end{pmatrix} \begin{pmatrix} 1 & 0 & \cdots & 0 \\ -1 & 1 & & \\ \vdots & & \ddots & \\ -1 & & & 1 \end{pmatrix} \in \mathbb{R}^{(r+1)\times(r+1)},$$

the continuity matrix

$$\mathcal{G}_h^n = \begin{pmatrix} 1 \\ 0 \\ \vdots \\ 0 \end{pmatrix} \left[\begin{pmatrix} 1, 0, \cdots, 0 \end{pmatrix} + B^T A^{-1} E \right] \in \mathbb{R}^{(r+1)\times(r+1)},$$

the mortality matrix

$$\mathcal{M}_{1h}^n = -\begin{pmatrix} 0 & & & \\ & {\mu_{11}}^n & & \\ & & \ddots & \\ & & & {\mu_{1r}}^n \end{pmatrix} \in \mathbb{R}^{(r+1)\times(r+1)},$$

and the division matrix

$$\mathcal{M}_{2h}^n = -\begin{pmatrix} 0 & & & \\ & \eta s\beta_1^n & & \\ & & \ddots & \\ & & & \eta s\beta_r^n \end{pmatrix} \in \mathbb{R}^{(r+1)\times(r+1)},$$

$$\mathcal{F}_{1h}^n = \begin{pmatrix} 0 & 2(1-f)\eta s h b_1\beta_1^n & \cdots & 2(1-f)\eta s h b_r\beta_r^n \\ 0 & 0 & \cdots & 0 \\ \vdots & \vdots & & \vdots \\ 0 & 0 & \cdots & 0 \end{pmatrix} \in \mathbb{R}^{(r+1)\times(r+1)}.$$

For $Q_h \in \mathcal{Z}_h$, we obtain the same matrices $\mathcal{E}_h^n$, $\mathcal{A}_h^n$, and $\mathcal{G}_h^n$, as well as the mortality matrix

$$\mathcal{M}_{3h}^n = -\begin{pmatrix} 0 & & & \\ & {\mu_{21}}^n & & \\ & & \ddots & \\ & & & {\mu_{2r}}^n \end{pmatrix} \in \mathbb{R}^{(r+1)\times(r+1)},$$

and the division matrix

$$\mathcal{F}_{2h}^n = \begin{pmatrix} 0 & 2f\eta s h b_1\beta_1^n & \cdots & 2f\eta s h b_r\beta_r^n \\ 0 & 0 & \cdots & 0 \\ \vdots & \vdots & & \vdots \\ 0 & 0 & \cdots & 0 \end{pmatrix} \in \mathbb{R}^{(r+1)\times(r+1)}.$$

Theorem 6.1. *Any age-semi-discrete solution of (2.7) is equivalently represented by the following differentiable functions: $P_h : [0,\infty) \to \mathbb{R}^{N(r+1)}$, $Q_h : [0,\infty) \to \mathbb{R}^{N(r+1)}$, and $N_h : [0,\infty) \to [0,\infty)$, such that*

$$\begin{cases} \hat{\mathcal{E}}_h \dfrac{\mathrm{d}P_h(t)}{\mathrm{d}t} = \left(\hat{\mathcal{A}}_h + \hat{\mathcal{G}}_h + \hat{\mathcal{M}}_{1h} + \left(\hat{\mathcal{F}}_{1h} + \hat{\mathcal{M}}_{2h}\right)\dfrac{N_h(t)}{H+N_h(t)}\right) P_h(t), \\ \hat{\mathcal{E}}_h \dfrac{\mathrm{d}Q_h(t)}{\mathrm{d}t} = \left(\hat{\mathcal{A}}_h + \hat{\mathcal{G}}_h + \hat{\mathcal{M}}_{3h} + \hat{\mathcal{F}}_{2h}\dfrac{N_h(t)}{H+N_h(t)}\right) Q_h(t), \\ \dfrac{\mathrm{d}N_h(t)}{\mathrm{d}t} = b\sigma - bN_h(t) - \dfrac{sN_h(t)}{H+N_h(t)} \sum_{n=0}^{N-1} h \sum_{i=1}^{r} b_i(P_h(t) + \gamma Q_h(t)), \\ (P_h(0), Q_h(0), N_h(0))^T = \mathcal{P}_h U_0, \end{cases} \tag{6.1}$$

where the matrices are defined as follows:

$$\hat{\mathcal{E}}_h = \mathrm{diag}\left(\mathcal{E}_h^0, \cdots, \mathcal{E}_h^{N-1}\right), \quad \hat{\mathcal{A}}_h = \mathrm{diag}\left(\mathcal{A}_h^0, \cdots, \mathcal{A}_h^{N-1}\right), \quad \hat{\mathcal{M}}_{1h} = \mathrm{diag}\left(\mathcal{M}_{1h}^0, \cdots, \mathcal{M}_{1h}^{N-1}\right),$$

$$\hat{\mathcal{M}}_{2h} = \mathrm{diag}\left(\mathcal{M}_{2h}^0, \cdots, \mathcal{M}_{2h}^{N-1}\right), \quad \hat{\mathcal{M}}_{3h} = \mathrm{diag}\left(\mathcal{M}_{3h}^0, \cdots, \mathcal{M}_{3h}^{N-1}\right),$$

$$\mathcal{G}_h = \begin{pmatrix} 0 & 0 & \cdots & 0 \\ \mathcal{G}_h^1 & 0 & \cdots & 0 \\ \vdots & \ddots & \ddots & \vdots \\ 0 & \cdots & \mathcal{G}_h^{N-1} & 0 \end{pmatrix}, \quad \hat{\mathcal{F}}_{1h} = \begin{pmatrix} \mathcal{F}_{1h}^0 & \cdots & \mathcal{F}_{1h}^{N-1} \\ 0 & \cdots & 0 \\ \vdots & & \vdots \\ 0 & \cdots & 0 \end{pmatrix}, \quad \hat{\mathcal{F}}_{2h} = \begin{pmatrix} \mathcal{F}_{2h}^0 & \cdots & \mathcal{F}_{2h}^{N-1} \\ 0 & \cdots & 0 \\ \vdots & & \vdots \\ 0 & \cdots & 0 \end{pmatrix}.$$

Proof. The proof is given in Appendix A.4. □

6.2. Time-full-discrete scheme

In this section, we discuss the time-full-discrete scheme based on (1.1). Denote the discrete time step size as ξ. Then, let $t_j = j\xi$ and P_h^j, Q_h^j, N_h^j be numerical approximations to $P_h(t_j)$, $Q_h(t_j)$, and $N_h(t_j)$, respectively. Then, an implicit-explicit scheme is written as

$$\begin{cases} \hat{\mathcal{E}}_h\left(\dfrac{P_h^{j+1}-P_h^j}{\xi}\right) = \hat{\mathcal{A}}_h P_h^{j+1} + \hat{\mathcal{G}}_h P_h^{j+1} + \hat{\mathcal{M}}_{1h} P_h^{j+1} + \hat{\mathcal{M}}_{2h}\dfrac{N_h^j}{H+N_h^j} P_h^{j+1} + \hat{\mathcal{F}}_{1h}\dfrac{N_h^j}{H+N_h^j} P_h^j, \\ \hat{\mathcal{E}}_h\left(\dfrac{Q_h^{j+1}-Q_h^j}{\xi}\right) = \hat{\mathcal{A}}_h Q_h^{j+1} + \hat{\mathcal{G}}_h Q_h^{j+1} + \hat{\mathcal{M}}_{3h} Q_h^{j+1} + \hat{\mathcal{F}}_{2h}\dfrac{N_h^j}{H+N_h^j} Q_h^j, \\ \dfrac{N_h^{j+1}-N_h^j}{\xi} = b\sigma - bN_h^{j+1} - \dfrac{sN_h^j}{H+N_h^j} hB^T(P_h^j + \gamma Q_h^j), \end{cases} \tag{6.2}$$

which is equivalent to

$$\begin{cases} \left(\hat{\mathcal{E}}_h - \xi\left(\hat{\mathcal{A}}_h + \hat{\mathcal{G}}_h + \hat{\mathcal{M}}_{1h} + \hat{\mathcal{M}}_{2h}\dfrac{N_h^j}{H+N_h^j}\right)\right) P_h^{j+1} = \left(\hat{\mathcal{E}}_h + \xi\hat{\mathcal{F}}_{1h}\dfrac{N_h^j}{H+N_h^j}\right) P_h^j, \\ \left(\hat{\mathcal{E}}_h - \xi\left(\hat{\mathcal{A}}_h + \hat{\mathcal{G}}_h + \hat{\mathcal{M}}_{3h}\right)\right) Q_h^{j+1} = \left(\hat{\mathcal{E}}_h + \xi\hat{\mathcal{F}}_{2h}\dfrac{N_h^j}{H+N_h^j}\right) Q_h^j, \\ (1+\xi b)N_h^{j+1} = \xi b\sigma + N_h^j - \dfrac{\xi sN_h^j}{H+N_h^j} hB^T(P_h^j + \gamma Q_h^j), \end{cases} \tag{6.3}$$

and the matrices $\hat{\mathcal{E}}_h - \xi\left(\hat{\mathcal{A}}_h + \hat{\mathcal{G}}_h + \hat{\mathcal{M}}_{1h} + \hat{\mathcal{M}}_{2h}\dfrac{N_h^j}{H+N_h^j}\right)$ and $\hat{\mathcal{E}}_h - \xi\left(\hat{\mathcal{A}}_h + \hat{\mathcal{G}}_h + \hat{\mathcal{M}}_{2h}\right)$ become the block-lower triangular matrices, whose invertibility is guaranteed by a sufficiently small time step $\xi > 0$.

Remark 6.2. *It is worth noting that if a classical implicit scheme is introduced, then the matrices* $\hat{\mathcal{E}}_h - \xi\left(\hat{\mathcal{A}}_h + \hat{\mathcal{G}}_h + \hat{\mathcal{M}}_{1h} + \hat{\mathcal{M}}_{2h}\dfrac{N_h^j}{H+N_h^j}\right)$ *and* $\hat{\mathcal{E}}_h - \xi\left(\hat{\mathcal{A}}_h + \hat{\mathcal{G}}_h + \hat{\mathcal{M}}_{2h}\right)$ *are changed into the matrices* $\hat{\mathcal{E}}_h - \xi\left(\hat{\mathcal{A}}_h + \hat{\mathcal{G}}_h + \hat{\mathcal{M}}_{3h} + \hat{\mathcal{F}}_{2h}\dfrac{N_h^j}{H+N_h^j}\right)$ *and* $\hat{\mathcal{E}}_h - \xi\left(\hat{\mathcal{A}}_h + \hat{\mathcal{G}}_h + \hat{\mathcal{M}}_{1h} + \left(\hat{\mathcal{M}}_{2h} + \hat{\mathcal{F}}_{1h}\right)\dfrac{N_h^j}{H+N_h^j}\right)$, *where they are block-Leslie matrices. It is a little harder to determine the regularity of the matrices. Moreover, even for a regular matrix, the computational cost increases as the age step size decreases.*

Theorem 6.2. *Under the condition in Theorem 5.2, the full-discrete scheme (6.2) shares the threshold of age-semi-discrete system (2.7), that is, the numerical solutions* P_h^j, Q_h^j, N_h^j *are asymptotically stable if and only if* $R_h < 1$*; on the contrary, the numerical solutions are unstable if and only if* $R_h > 1$.

Proof. The proof is given in Appendix A.5. □

Remark 6.3. *Biologically, the condition* $R_h < 1$ *means that a sufficiently small tumor cell population cannot maintain its growth and tends to disappear. When* $R_h > 1$*, the tumor-free equilibrium loses stability, indicating that tumor cells may persist and continue to proliferate.*

The preceding sections establish the convergence of the numerical basic reproduction number R_h to R_0 and show that R_h serves as a stability threshold for both the age-semi-discrete and full-discrete systems. To illustrate these theoretical results and assess the practical performance of the proposed numerical methods, we next present several numerical examples.

7. Numerical examples

In this section, we will give several examples to demonstrate the conclusions on convergence and stability we obtained above.

7.1. Convergence

Example 7.1. *Consider the following functions given by [27], that is,*

$$\begin{aligned} \beta(a) &= \begin{cases} 0, & 0 \le a \le a_1, \\ \dfrac{1}{\varrho} \dfrac{(a-a_1)^2}{2\varrho^2 + 2\varrho(a-a_1) + (a-a_1)^2}, & a > a_1 \end{cases} \\ \mu_1(a) &= \begin{cases} \mu, & 0 \le a \le a_1, \\ \mu + \mu(a-a_1)^2, & a > a_1, \end{cases} \end{aligned} \tag{7.1}$$

where $\mu = 0.268$, $\varrho = 2$ is a variance constant, and $a_1 = 25$ is the age at which proliferating cells begin to divide. Here, $\mu_1(a)$ denotes the age-dependent mortality rate of proliferating cells. Since the computation and convergence analysis of R_h involve only $\mu_1(a)$, the function $\mu_2(a)$ is not required in this example.

We use the same method as in [28] to calculate the convergence order. According to Theorem 4.1, if numerical methods satisfy the orthogonality condition

$$J_\nu = \int_0^1 s^\nu \prod_{i=1}^{r} (s - c_i)\, \mathrm{d}s = 0, \quad \nu = 0, 1, \cdots, \kappa - 1, \quad \kappa = 1, 2, \cdots, r,$$

the numerical basic reproduction numbers must be a superconvergence, that is, the convergence order is higher than r. It is shown that the numerical basic reproduction numbers converge with accuracy of order $2, 4, 1, 3$ *for* 1-*Gauss,* 2-*Gauss,* 1-*Radau IIA, and* 2-*Radau IIA methods in Table 2.*

Table 2. Convergence orders for numerical methods.

convergence order / methods / h	1-Gauss	2-Gauss	1-Radau IIA	2-Radau IIA
0.1	1.9991	3.9993	1.0536	2.9921
0.05	1.9998	3.9998	1.0272	2.9963
0.025	1.9999	3.9987	1.0137	2.9982
0.0125	2.0000	4.0285	1.0069	2.9991
0.00625	2.0000	4.1624	1.0034	2.9996

Remark 7.1. *The slight increase in the observed convergence order beyond the theoretical value 4 for*

the 2-Gauss method at very small values of h is caused by the influence of round-off errors and does not contradict our theoretical estimates.

7.2. Stability

In this subsection, we separately discuss the stability of β as a constant function and β as a function related to a.

Example 7.2. *To consider the stability of system (1.1), we discuss the influence of some parameters on the solutions of the model, namely the evolution speed k, the proportion f, and the conversion factor η. The parameters are taken from [29] as follows:*

$$b = 1.0, \;\; s = 0.1346, \;\; H = 0.1, \;\; \gamma = 0.1, \;\; \sigma = 2$$

and the others are assumed to be as follows:

$$\mu_1 = \mu_2 = 0.03, \;\; \beta = 0.09.$$

To investigate the stability of numerical solutions, we first consider the relationship among R_h and f, k, η. Figure 1(a) shows that the larger cancer cell evolution speed needs the smaller conversion factor to guarantee the condition $R_h < 1$. Figure 1(b) suggests that the more newborn cancer cells turn into quiescent cells, the larger the conversion factor needs to be to guarantee the condition $R_h < 1$. Figure 1(c) identifies the stable region as f and k vary.

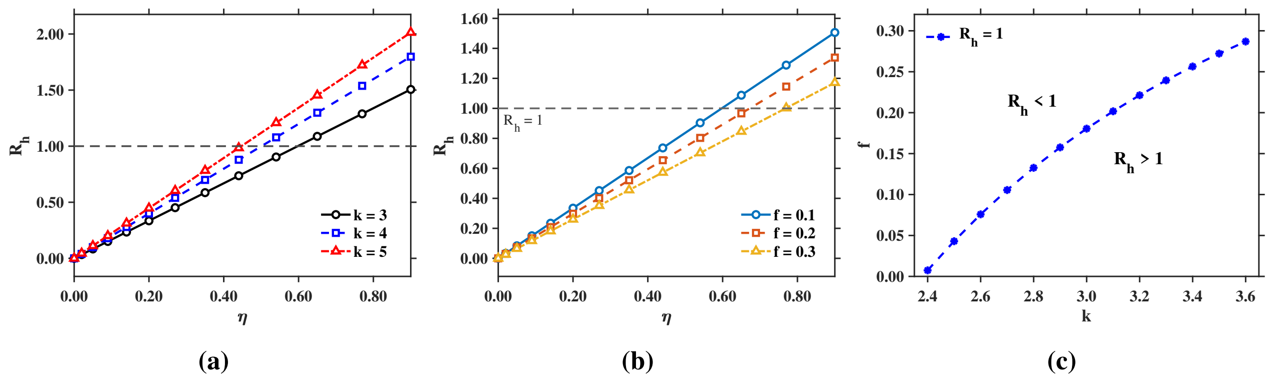

Figure 1. (a) The effect of η on R_h with $f = 0.1$ under the different evolution speeds $k = 3$, $k = 4$, and $k = 5$. (b) The effect of η on R_h with $k = 3$ under the differential proportion $f = 0.1$, $f = 0.2$, and $f = 0.3$. (c) The effect of f on $R_h - 1$ with $\eta = 0.8$ as k increases.

From Theorem 6.2, we know that the numerical solutions are asymptotically stable if $R_h < 1$, which means that the number of tumor cells is decreasing and eventually disappears when the initial tumor population is sufficiently small. When $R_h > 1$, the numerical solutions are unstable, which means the tumor population may persist and increase. The parameter settings and the corresponding values of R_h for the one-stage and two-stage collocation methods are summarized in Table 3. Figures 2 and 3 suggest that the tumor population dies out if $R_h < 1$. Figures 4 and 5 suggest that the tumor population increases if $R_h > 1$.

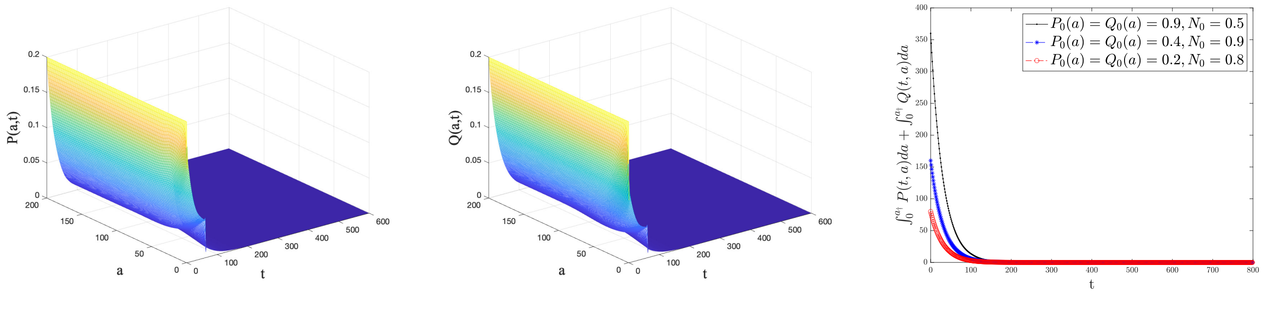

(a) **(b)** **(c)**

Figure 2. (a) The numerical distribution of $P(t, a)$ with $r = 1$ for $R_h < 1$. (b) The numerical distribution of $Q(t, a)$ with $r = 1$ for $R_h < 1$. (c) The time series of the total population $\int_0^{a_\dagger} P(t, a)\mathrm{d}a + \int_0^{a_\dagger} Q(t, a)\mathrm{d}a$ under three different initial values. The initial values of (a) and (b) are as follows: $(P_0(a), Q_0(a), N_0) = (0.2, 0.2, 0.8)$.

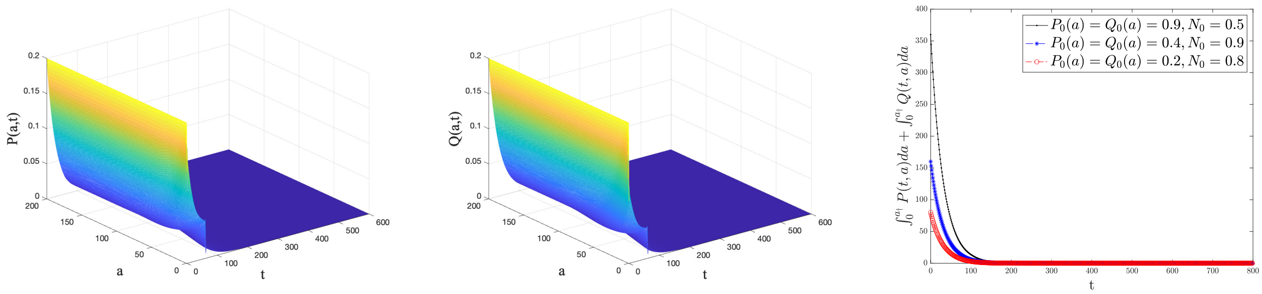

(a) **(b)** **(c)**

Figure 3. (a) The numerical distribution of $P(t, a)$ with $r = 2$ for $R_h < 1$. (b) The numerical distribution of $Q(t, a)$ with $r = 2$ for $R_h < 1$. (c) The time series of the total population $\int_0^{a_\dagger} P(t, a)\mathrm{d}a + \int_0^{a_\dagger} Q(t, a)\mathrm{d}a$ under three different initial values. The initial values of (a) and (b) are as follows: $(P_0(a), Q_0(a), N_0) = (0.2, 0.2, 0.8)$.

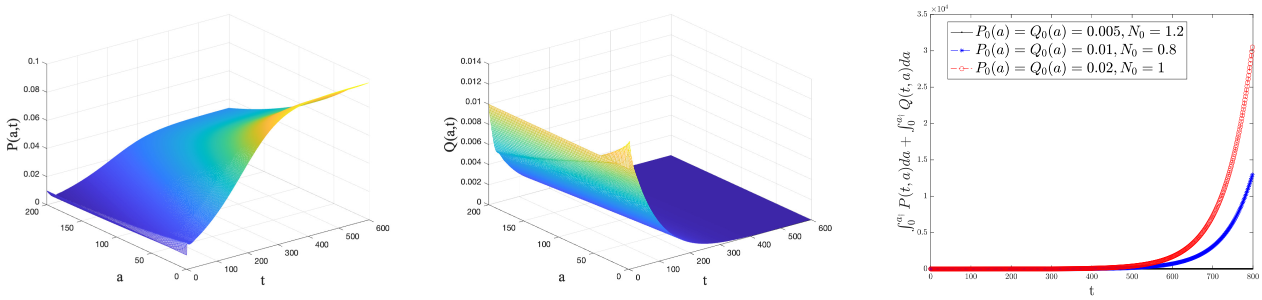

(a) **(b)** **(c)**

Figure 4. (a) The numerical distribution of $P(t, a)$ with $r = 1$ for $R_h > 1$. (b) The numerical distribution of $Q(t, a)$ with $r = 1$ for $R_h > 1$. (c) The time series of the total population $\int_0^{a_\dagger} P(t, a)\mathrm{d}a + \int_0^{a_\dagger} Q(t, a)\mathrm{d}a$ under three different initial values. The initial values of (a) and (b) are as follows: $(P_0(a), Q_0(a), N_0) = (0.01, 0.01, 0.4)$.

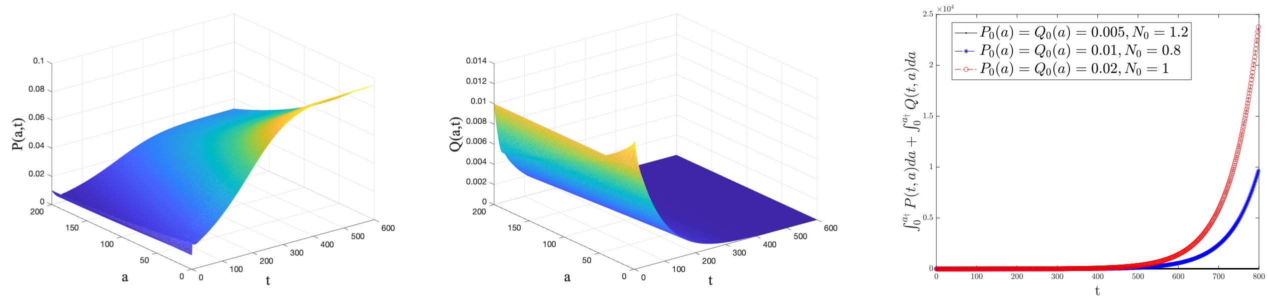

(a) **(b)** **(c)**

Figure 5. (a) The numerical distribution of $P(t, a)$ with $r = 2$ for $R_h > 1$. (b) The numerical distribution of $Q(t, a)$ with $r = 2$ for $R_h > 1$. (c) The time series of the total population $\int_0^{a_\dagger} P(t, a)\mathrm{d}a + \int_0^{a_\dagger} Q(t, a)\mathrm{d}a$ under three different initial values. The initial values of (a) and (b) are as follows: $(P_0(a), Q_0(a), N_0) = (0.01, 0.01, 0.4)$.

Table 3. Parameter settings and corresponding values of R_h.

Parameters			R_h	
k	f	η	$r = 1$	$r = 2$
1.1	0.4	0.3	0.0605	0.0603
7.0	0.4	0.9	1.8284	1.8286

Remark 7.2. *Figure 1 illustrates how the physiological age evolution speed k, the fraction f of newborn cells entering the quiescent state, and the nutrient-to-tumor conversion factor η affect the reproductive potential of tumor cells, as characterized by R_h. Variations in these biologically relevant parameters may move the system across the threshold $R_h = 1$. Figures 2 and 3 show that, when $R_h < 1$, the densities of both proliferating and quiescent tumor cells, as well as the total tumor cell population, gradually decrease under different initial conditions. Biologically, this means that a sufficiently small tumor cell population cannot maintain its growth and eventually tends to disappear. In contrast, Figures 4 and 5 show that, when $R_h > 1$, the tumor-free equilibrium loses stability, and the proliferating and quiescent tumor cell populations may persist and increase. The consistent qualitative behavior obtained for $r = 1$ and $r = 2$ also indicates that the threshold property is preserved by both collocation schemes.*

Example 7.3. *According to Remark 5.2, consider the function $\beta(a)$ given by (7.1), take $f = 0.5$, $k = 1.1$, and $\eta = 0.1$, and other parameters are as stated above; we can obtain the numerical solution when $R_h < 1$ with $r = 1$ and $r = 2$ in Figures 6 and 7. Take $f = 0.2$, $k = 5$, and $\eta = 0.2$ and other parameters are as above; we can obtain the numerical solution when $R_h > 1$ with $r = 1$ and $r = 2$ in Figures 8 and 9. However, the current theoretical proof only provides the case under implicit Euler methods.*

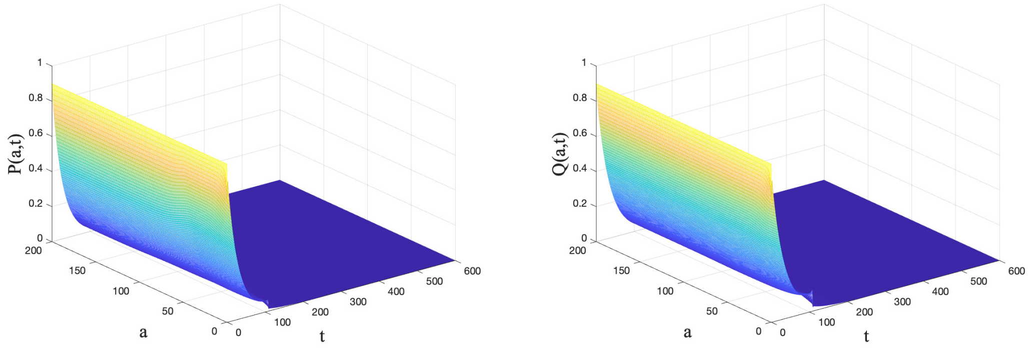

(a) **(b)**

Figure 6. (a) The numerical distribution of $P(t, a)$ with $r = 1$ for $R_h < 1$. (b) The numerical distribution of $Q(t, a)$ with $r = 1$ for $R_h < 1$. The initial values of (a) and (b) are as follows: $(P_0(a), Q_0(a), N_0) = (0.9, 0.9, 0.5)$.

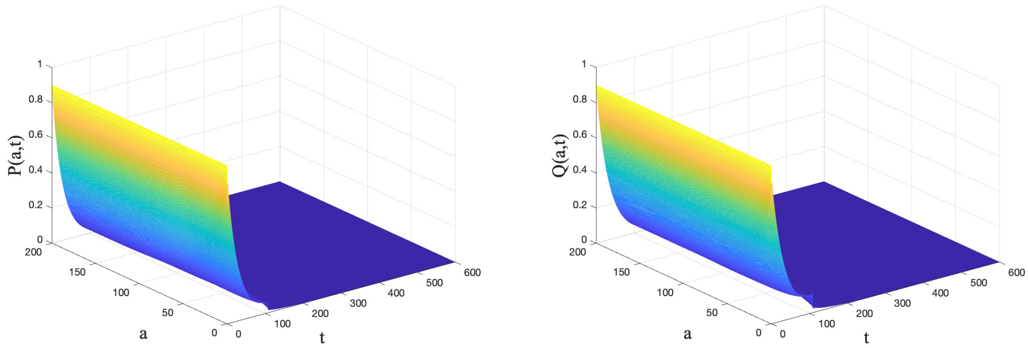

(a) **(b)**

Figure 7. (a) The numerical distribution of $P(t, a)$ with $r = 2$ for $R_h < 1$. (b) The numerical distribution of $Q(t, a)$ with $r = 2$ for $R_h < 1$. The initial values of (a) and (b) are as follows: $(P_0(a), Q_0(a), N_0) = (0.9, 0.9, 0.5)$.

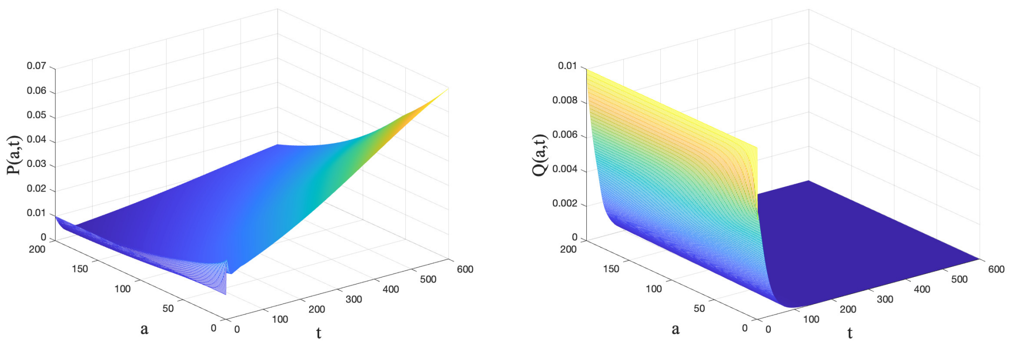

(a) **(b)**

Figure 8. (a) The numerical distribution of $P(t, a)$ with $r = 1$ for $R_h > 1$. (b) The numerical distribution of $Q(t, a)$ with $r = 1$ for $R_h > 1$. The initial values of (a) and (b) are as follows: $(P_0(a), Q_0(a), N_0) = (0.01, 0.01, 0.4)$.

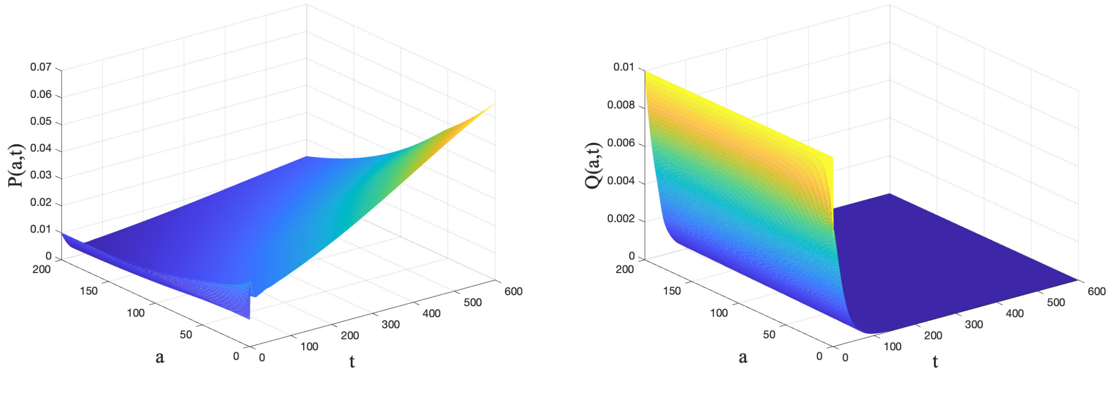

(a) **(b)**

Figure 9. (a) The numerical distribution of $P(t, a)$ with $r = 2$ for $R_h > 1$. (b) The numerical distribution of $Q(t, a)$ with $r = 2$ for $R_h > 1$. The initial values of (a) and (b) are as follows: $(P_0(a), Q_0(a), N_0) = (0.01, 0.01, 0.4)$.

Remark 7.3. *Figures 6–9 provide a biological interpretation of the threshold R_h when the division rate depends on cell age. Figures 6 and 7 show that both proliferating and quiescent tumor cell populations tend to disappear when $R_h < 1$, indicating that age-dependent cell division is insufficient to maintain the growth of a sufficiently small tumor population. Figures 8 and 9 show that the tumor cell populations may persist and grow when $R_h > 1$. Therefore, the numerical results suggest that the threshold role of R_h remains valid even when the heterogeneity of the cell-division process with respect to age is taken into account. The results obtained with $r = 1$ and $r = 2$ exhibit the same qualitative biological behavior.*

Example 7.4. *In this numerical example, we compare the continuous collocation method with the spectral method. As shown in Figures 10 and 11, when k is large, the spectral method produces negative solutions, while under the same coefficients, the continuous collocation method can maintain the nonnegativity of numerical solutions. Such nonnegativity is a crucial requirement for biologically meaningful numerical solutions, which the continuous collocation method satisfies.*

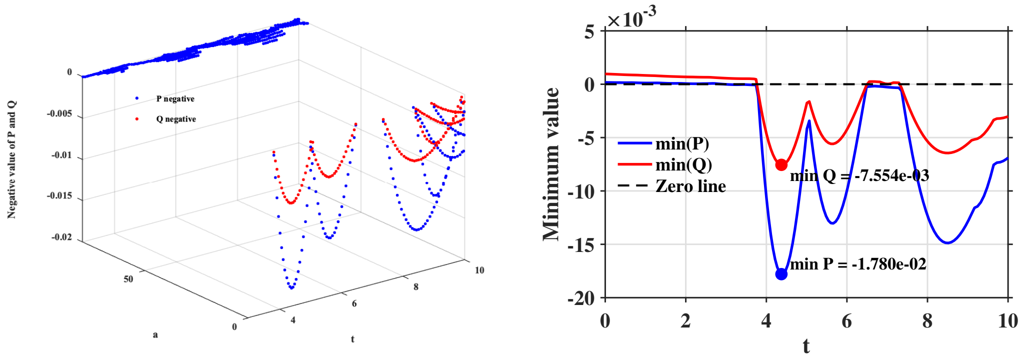

(a) **(b)**

Figure 10. (a) The negative regions with spectral method in $P(t, a)$ and $Q(t, a)$ when $k = 10$. (b) Minimum values of $P(t, a)$ and $Q(t, a)$ that vary over time when $k = 10$.

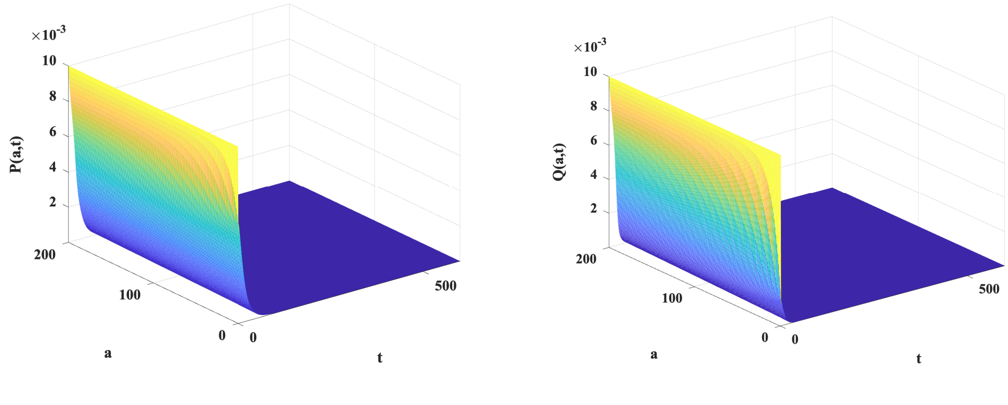

Figure 11. (a) The numerical distribution of $P(t, a)$ with the continuous collocation method when $k = 10$. (b) The numerical distribution of $Q(t, a)$ with the continuous collocation method when $k = 10$.

Remark 7.4. *Figure 10 shows that the spectral method produces negative values of proliferating and quiescent cell densities when* $k = 10$*. Such negative values are biologically inadmissible because cell population densities must remain nonnegative. Under the same parameter setting, Figure 11 shows that the continuous collocation method preserves the nonnegativity of both cell populations. Therefore, the continuous collocation method produces numerical solutions that are more consistent with the biological meaning of the age-structured tumor model.*

8. Conclusions

This paper is concerned with the study of the numerical stability of a nonlinear age-structured tumor cell population model. With the theory of continuous collocation methods, the numerical basic reproduction number R_h is obtained. Moreover, it is also a threshold for the local stability of age-semi-discrete scheme, which is not a quadrature for the exact basic reproduction number but converges to the exact one with at least $r + 1$ order accuracy. Finally, four numerical experiments are given to verify the above conclusions. From a biological perspective, the threshold R_h characterizes whether a small tumor cell population can maintain its growth in the given nutrient environment. When $R_h < 1$, the tumor-free equilibrium is locally asymptotically stable, indicating that a sufficiently small tumor cell population tends to disappear. In contrast, when $R_h > 1$, the tumor-free equilibrium loses stability, and tumor cells may persist and continue to proliferate. The threshold results may also provide qualitative insights into potential tumor treatment strategies. In the framework of the present model, therapeutic interventions that suppress the proliferative capacity of tumor cells, increase tumor-cell mortality, prolong the cell-division time, or restrict nutrient-supported tumor growth may reduce the reproduction potential of tumor cells and help shift the system toward the regime $R_h < 1$. Therefore, the threshold R_h may serve as a qualitative indicator for comparing the effects of different intervention mechanisms. Nevertheless, the present model is a simplified theoretical framework, and further parameter estimation, sensitivity analysis, and clinical validation are required before the results can be applied to practical treatment design. The present model focuses on age-structured tumor dynamics without considering the spatial movement of tumor cells. In future work, we will extend the model by incorporating reaction-diffusion terms to investigate the effects of spatial heterogeneity and cell migration.

Author contributions

Hefan Yin: Formal analysis, Investigation, Writing–original draft; Jianfang Gao: Conceptualization, Validation, Funding acquisition, Writing–review and editing; Zhanwen Yang: Methodology, Writing–review and editing. All authors have read and agreed to the published version of the manuscript.

Use of Generative-AI tools declaration

The authors declare they have not used Artificial Intelligence (AI) tools in the creation of this article.

Acknowledgments

This project is supported by the Doctoral Innovation Project of Harbin Normal University (HSDBSCX2025-16), the open research fund of Heilongjiang Key Laboratory of Analysis on Machine Learning and Dynamic System (HLJKL2505) and the Natural Science Foundation of Heilongjiang Province (PL2025A007).

Conflict of interest

The authors declare that they have no conflict of interest.

References

1. G. Bell, E. Anderson, Cell growth and division, I. A mathematical model with applications to cell volume distributions in mammalian suspension cultures, *Biophys. J.*, **7** (1967), 329–351. http://doi.org/10.1016/S0006-3495(67)86592-5

2. G. Bell, Cell growth and division, III. Conditions for balanced exponential growth in a mathematical model, *Biophys. J.*, **8** (1968), 431–444. http://doi.org/10.1016/S0006-3495(68)86498-7

3. W. Li, X. Liu, Y. Lang, Numerical analysis of a nonlinear age-structured HBV model with saturated incidence and spatial diffusion, *Math. Comput. Simul.*, **225** (2024), 250–266. http://doi.org/10.1016/j.matcom.2024.05.022

4. K. Kuritz, D. Stöhr, N. Pollak, F. Allgöwer, On the relationship between cell cycle analysis with ergodic principles and age-structured cell population models, *J. Theor. Biol.*, **414** (2017), 91–102. http://doi.org/10.1016/j.jtbi.2016.11.024

5. M. Doumic, A. Marciniak-Czochra, B. Perthame, J. Zubelli, A structured population model of cell differentiation, *SIAM J. Appl. Math.*, **71** (2011), 1918–1940. http://doi.org/10.1137/100816584

6. S. Zhang, P. Wu, S. Liu, Spatiotemporal evolution of a pine wilt disease model integrating infectious disease transmission and predator–prey interactions, *J. Math. Biol.*, **92** (2026), 83. http://doi.org/10.1007/s00285-026-02406-1

7. S. Yang, X. Liu, Numerical threshold stability analysis of a positivity-preserving IMEX numerical scheme for a nonlinear age-space structured SIR epidemic model, *Comput. Appl. Math.*, **43** (2024), 240. http://doi.org/10.1007/s40314-024-02768-6

8. J. Li, G. Xu, N. Liu, D. Wang, H. Yang, Stability analysis and Hopf bifurcation in a delayed nonlinear tumor-macrophage model, *Phys. Scr.*, **100** (2025), 035222. http://doi.org/10.1088/1402-4896/adb34c

9. P. Wu, S. Zhang, X. Wang, H. Wang, Spatiotemporal cholera dynamics with antibiotic resistance and vaccination via demographic-epidemic data in Zimbabwe, *J. Math. Biol.*, **92** (2026), 42. http://doi.org/10.1007/s00285-026-02360-y

10. N. Liu, G. Xu, H. Yang, Stability and Hopf bifurcation analysis in a fractional-order delayed tumor-macrophage model, *Int. J. Dyn. Control*, **13** (2025), 77. http://doi.org/10.1007/s40435-024-01575-5

11. G. Webb, *Theory of Nonlinear Age-Dependent Population Dynamics*, New York: Dekker, 1985.

12. J. Dyson, R. Villella-Bressan, G. F. Webb, Asynchronous exponential growth in an age structured population of proliferating and quiescent cells, *Math. Biosci.*, **177** (2002), 73–83. http://doi.org/10.1016/S0025-5564(01)00097-9

13. C. Liu, X. Liu, Y. Wang, Y. Wei, Dynamics of an age-structured tumor cell population model with nutrition, *Nonlinear Dyn.*, **112** (2024), 19561–19587. http://doi.org/10.1007/s11071-024-10034-x

14. Z. Liu, C. Guo, H. Li, L. Zhao, Analysis of a nonlinear age-structured tumor cell population model, *Nonlinear Dyn.*, **98** (2019), 283–300. http://doi.org/10.1007/s11071-019-05190-4

15. N. Mantzaris, P. Daoutidis, F. Srienc, Numerical solution of multi-variable cell population balance models: I. Finite difference methods, *Comput. Chem. Eng.*, **25** (2001), 1411–1440. http://doi.org/10.1016/S0098-1354(01)00709-8

16. N. Mantzaris, P. Daoutidis, F. Srienc, Numerical solution of multi-variable cell population balance models. III. Finite element methods, *Comput. Chem. Eng.*, **25** (2001), 1463–1481. http://doi.org/10.1016/S0098-1354(01)00711-6

17. Z. Jackiewicz, B. Zubik-Kowal, B. Basse, Finite-difference and pseudo-spectral methods for the numerical simulations of in vitro human tumor cell population kinetics, *Math. Biosci. Eng.*, **6** (2009), 561–572. http://doi.org/10.3934/mbe.2009.6.561

18. V. Akimenko, F. Adi-Kusumo, Age-structured delayed SIPCV epidemic model of HPV and cervical cancer cells dynamics I. Numerical method, *Biomath.*, **10** (2021), 2110027. http://doi.org/10.11145/j.biomath.2021.10.027

19. S. Franz, N. Kopteva, On the solution existence for collocation discretizations of time-fractional subdiffusion equations, *J. Sci. Comput.*, **100** (2024), 68. http://doi.org/10.1007/s10915-024-02619-w

20. S. D. Reggi, F. Scarabel, R. Vermiglio, On the convergence of the pseudospectral approximation of reproduction numbers for age-structured models, *SIAM J. Numer. Anal.*, **64** (2026), 1073–1094. http://doi.org/10.1137/24M1687224

21. D. Breda, S. D. Reggi, R. Vermiglio, A numerical method for the stability analysis of linear age-structured models with nonlocal diffusion, *SIAM J. Sci. Comput.*, **46** (2024), A953–A973. http://doi.org/10.1137/23M1568971

22. O. Angulo, J. Lopez-Marcos, M. Lopez-Marcos, J. Martinez-Rodriguez, Numerical analysis of an open marine population model with spaced-limited recruitment, *Math. Comput. Model.*, **52** (2010), 1037–1044. http://doi.org/10.1016/j.mcm.2010.02.020

23. E. Hairer, C. Lubich, G. Wanner, *Geometric Numerical Integration. Structure-Preserving Algorithms for Ordinary Differential Equations*, New York: Springer, 2006.

24. D. Breda, M. Iannelli, S. Maset, R. Vermiglio, Stability analysis of the gurtin-maccamy model, *SIAM J. Numer. Anal.*, **46** (2008), 980–995. http://doi.org/10.1137/070685658

25. E. Hairer, G. Wanner, *Solving Ordinary Differential Equations II: Stiff and Differential-Algebraic Systems*, New York: Springer, 1996.

26. B. Hermann, *Collocation Methods for Volterra Integral and Related Functional Differential Equations*, Cambridge: Cambridge University Press, 2004.

27. Z. Liu, J. Chen, J. Pang, P. Bi, S. Ruan, Modeling and analysis of a nonlinear age-structured model for tumor cell populations with quiescence, *J. Nonlinear Sci.*, **28** (2018), 1763–1791. http://doi.org/10.1007/s00332-018-9463-0

28. M. Li, Z. Yang, Numerical analysis of an age-structured model for HIV viral dynamics with latently infected T cells based on collocation methods, *Math. Comput. Simul.*, **230** (2025), 289–305. http://doi.org/10.1016/j.matcom.2024.09.028

29. D. Gammacke, H. Byrne, C. Lewis, Estimating the selective advantage of mutant p53 tumour cells to repeated rounds of hypoxia, *Bull. Math. Biol.*, **63** (2001), 135–166. http://doi.org/10.1006/bulm.2000.0210

30. J. B. Conway, *Function of One Complex Variable*, Berlin: Springer, 1978.

A. Appendix

A.1. Proof of Theorem 4.1

According to the quadrature formula with $\{c_i\}$, we obtain

$$I_1 = \sum_{n=0}^{N-1} \left| h \sum_{i=1}^{r} b_i \beta_i^n \hat{\varphi}_{hi}^n - \int_{a_n}^{a_{n+1}} \beta(a) \hat{\varphi}_h(a) \, \mathrm{d}a \right| = \sum_{n=0}^{N-1} h \left| \sum_{i=1}^{r} b_i \beta_i^n \hat{\varphi}_{hi}^n - \int_0^1 \beta(a_n + vh) \hat{\varphi}_h(a_n + vh) \, \mathrm{d}v \right|.$$

If $\{c_i\}$ satisfies the orthogonality condition J_v, then

$$I_1 \leq \sum_{n=0}^{N-1} h C_1 h^{r+\kappa} = a_\dagger C_1 h^{r+\kappa}.$$

Next we consider the collocation error. Let

$$\delta_h(a) = -k\hat{\varphi}_h'(a) - \left(\mu_1(a) + \frac{\eta s\beta(a)\sigma}{H+\sigma}\right)\hat{\varphi}_h(a),$$

where $\delta_h(a) = 0, a \in \mathcal{M}_h, \delta_h \in C^{r+\kappa}(0,\infty)$. Then, $e_h = \hat{\varphi} - \hat{\varphi}_h$ satisfies

$$\begin{cases} ke_h'(a) = -\left(\mu_1(a) + \dfrac{\eta s\beta(a)\sigma}{H+\sigma}\right)e_h(a) + \delta_h(a), \quad a \in [0, a_\dagger], \\ e_h(0) = 0, \end{cases}$$

whose solution is given by

$$e_h(a) = \frac{1}{k}\int_0^a r(a,s)\delta_h(s)\,\mathrm{d}s, \quad a \in [0, a_\dagger], \tag{A.1}$$

where $r(a,s) = e^{\frac{1}{k}\int_a^s\left(\mu_1(\tau)+\frac{\eta s\beta(\tau)\sigma}{H+\sigma}\right)\mathrm{d}\tau}$. According to (A.1), we have

$$\begin{aligned} I_2 = \sum_{n=0}^{N-1}\left|\int_{a_n}^{a_{n+1}}\beta(a)(\hat{\varphi}_h(a) - \hat{\varphi}(a))\,\mathrm{d}a\right| \le \sum_{n=0}^{N-1}\int_{a_n}^{a_{n+1}}\beta(a)\left|e_h(a)\right|\,\mathrm{d}a &= \frac{1}{k}\int_0^{a_\dagger}\left|\delta_h(s)K(s)\right|\,\mathrm{d}s \\ &= \frac{1}{k}\left|\sum_{n=0}^{N-1}h\sum_{i=1}^{r}b_i\delta_h(a_n+c_ih)K(a_n+c_ih) + E_r\right|, \end{aligned}$$

where $K(s) = \int_s^{a_\dagger}\beta(a)r(a,s)\,\mathrm{d}a$, and E_r denotes the quadrature error obtained from the quadrature formula. If $\{c_i\}$ satisfies the orthogonality condition J_v, then

$$|E_r| \le C_2h^{r+\kappa}, \quad 1 \le \kappa \le r.$$

Because of $\delta_h(a_n + c_ih) = 0$, we have

$$I_2 \le \frac{1}{k}|E_r| \le \frac{1}{k}C_2h^{r+\kappa}.$$

Then the proof is complete.

A.2. Proof of Theorem 5.1

For $\lambda \in \partial B(\bar{\lambda}, \gamma_0)$, we have

$$|d(\lambda)| > C_2\left|\lambda - \bar{\lambda}\right|^v = C_2\gamma_0^v \ge C_1h^r \ge |d_h(\lambda) - d(\lambda)|.$$

Hence, by Rouché theorem in [30], d and d_h have exactly the same number of zeros counted with their multiplicities in $B(\bar{\lambda}, \gamma_0)$, satisfying

$$C_1h^r \ge |d_h(\lambda_h) - d(\lambda_h)| = |d(\lambda_h)| \ge C_2\left|\bar{\lambda} - \lambda_h\right|^v.$$

A.3. Proof of Theorem 5.2

To consider the stability condition of nonlinear system (2.7), we linearize it to (3.1) and consider the stability of linear system (3.1) instead of (2.7). Additionally, let λ_h be the zeros of $d_h(\lambda)$, which is independent of h. Define $d_h(\lambda_h) = 1 - S_h$, that is, $S_h = \dfrac{2(1-f)\eta s\sigma}{H+\sigma}\sum_{n=0}^{N-1} h \sum_{i=1}^{r} b_i \beta_i^n \hat{\varphi}_h(a_i^n, \lambda_h) = 1$. It is necessary to explain that $|\lambda_h|$ is finite. Otherwise, S_h, based on continuous collocation methods, tend to zero. We can see that $d_h(\lambda_h)$ is only related to the function $\hat{\varphi}_h\left(a_i^n, \lambda_h\right)$, so we consider the system (3.3) with Runge-Kutta methods where the coefficient satisfies Lemma 2.1.

Assume that $\beta(a) = \beta^*$, then we organize (3.3) into the following form:

$$\begin{cases} \lambda_h \hat{\varphi}_h = -k\hat{\varphi}_h' - \mu_1(a)\hat{\varphi}_h - \dfrac{\eta s \beta^* \sigma}{H+\sigma}\hat{\varphi}_h, \quad a \in \mathcal{M}_h, \\ \hat{\varphi}_h(0) = 1, \end{cases} \tag{A.2}$$

because of $0 < \mu_- \leq \mu_i(a) \leq \mu_+$ in assumption (1.2), then we have

$$\begin{aligned} -k\hat{\varphi}_h' - \mu_1(a)\hat{\varphi}_h - \frac{\eta s \beta^* \sigma}{H+\sigma}\hat{\varphi}_h &= -k\hat{\varphi}_h' - \mu_+\hat{\varphi}_h - \frac{\eta s \beta^* \sigma}{H+\sigma}\hat{\varphi}_h + \mu_+\hat{\varphi}_h - \mu_1(a)\hat{\varphi}_h \\ &= L_h\hat{\varphi}_h + N_h\hat{\varphi}_h, \end{aligned} \tag{A.3}$$

where

$$L_h\hat{\varphi}_h = -k\hat{\varphi}_h' - \mu_+\hat{\varphi}_h - \frac{\eta s \beta^* \sigma}{H+\sigma}\hat{\varphi}_h$$

and $N_h\hat{\varphi}_h = \mu_+\hat{\varphi}_h - \mu_1(a)\hat{\varphi}_h$.

First, for $N_h\hat{\varphi}_h = \mu_+\hat{\varphi}_h - \mu_1(a)\hat{\varphi}_h$, we have

$$\|\mu_+\hat{\varphi}_h - \mu_1(a)\hat{\varphi}_h\| \leq (\mu_+ - \mu_-)\|\hat{\varphi}_h\|,$$

so the spectral radius of $N_h\hat{\varphi}_h$ must be bounded. Next, we only need to consider whether the spectral radius of $L_h\hat{\varphi}_h$ is bounded.

For $L_h\hat{\varphi}_h = \lambda_h\hat{\varphi}_h$, we obtain

$$\begin{cases} \hat{\varphi}_h' = -\dfrac{1}{k}\left(\mu_+ + \dfrac{\eta s \beta^* \sigma}{H+\sigma} + \lambda_h\right)\hat{\varphi}_h, \quad a \in \mathcal{M}_h, \\ \hat{\varphi}_h(0) = 1, \end{cases} \tag{A.4}$$

for convenience, we define $\hat{\varphi}_h' = -\delta(\lambda_h)\hat{\varphi}_h$, where $\delta(\lambda_h) = \dfrac{1}{k}\left(\mu_+ + \dfrac{\eta s \beta^* \sigma}{H+\sigma} + \lambda_h\right)$; then, we obtain the following numerical scheme by Runge-Kutta methods:

$$\begin{cases} \hat{\varphi}_h(a_{n+1}, \lambda_h) = \hat{\varphi}_h(a_n) + h\sum_{i=1}^{r} b_i\left(-\delta(\lambda_h)\right)\Phi_h(a_i^n, \lambda_h), \\ \Phi_h(a_i^n, \lambda_h) = \hat{\varphi}_h(a_n) + h\sum_{j=1}^{m} a_{ij}\left(-\delta(\lambda_h)\right)\Phi_h(a_j^n, \lambda_h), \end{cases} \tag{A.5}$$

where $i = 1, \cdots, r$, $n = 0, \cdots, N-1$, $j = 1, \cdots, r$, and $\Phi_h(a_i^n, \lambda_h) = \hat{\varphi}_h\left(a_i^n, \lambda_h\right)$ are the collocation solutions of (A.2). Then, we have

$$\begin{aligned} &\Phi_h(a_i^n, \lambda_h) = \left(I + h\delta(\lambda_h)A\right)^{-1}\hat{\varphi}_h(a_n, \lambda_h)e, \\ &\hat{\varphi}_h(a_n, \lambda_h) = \hat{\varphi}_h(0)\left(1 - h\delta(\lambda_h)B^T\left(I + h\delta(\lambda_h)A\right)^{-1}e\right)^n, \end{aligned} \tag{A.6}$$

where $i = 1, \cdots, r$, $A = (a_{ij})_{r\times r}$, $B = (b_1, b_2, \cdots, b_r)^T$, $e = (1, 1, \cdots, 1)^T \in \mathbb{R}^{r\times 1}$ and I is a r-order identity matrix. Therefore,

$$\Phi_h(a_i^n, \lambda_h) = (I + h\delta(\lambda_h) A)^{-1} \left(1 - h\delta(\lambda_h) B^T (I + h\delta(\lambda_h) A)^{-1} e\right)^n e.$$

Let $R(z) = 1 + zB^T (I - zA)^{-1} e$, where $z = -h\delta(\lambda_h)$. Because Runge-Kutta methods are algebraically stable, then $|R(z)| \le 1$. Therefore, we obtain

$$\begin{aligned} S_h &= \frac{2(1-f)\eta s\sigma}{H+\sigma} \sum_{n=0}^{N-1} h\beta^* B^T \hat{\varphi}_h(a_i^n, \lambda_h) = \frac{2(1-f)\eta s\sigma}{H+\sigma} \sum_{n=0}^{N-1} h\beta^* B^T \Phi_h(a_i^n, \lambda_h) \\ &= \frac{2(1-f)\eta s\sigma}{H+\sigma} \sum_{n=0}^{N-1} h\beta^* B^T (I - zA)^{-1} e\,(R(z))^n \\ &= \frac{2(1-f)k\eta s\sigma}{H+\sigma} \beta^* \frac{1-(R(z))^N}{\left(\mu_+ + \dfrac{\eta s\beta^*\sigma}{H+\sigma} + \lambda_h\right)} \to 0, \quad \lambda_h \to \infty, \end{aligned}$$

which means $d_h(\lambda_h) = 1$, which is a contradiction. Then, we obtain that λ_h is finite. Denote $|\lambda_h| \le \Lambda$.

If $R_h < 1 - \delta$ ($\delta > 0$ is sufficiently small), then according to Lemma 5.1, the fact that $R_0 < 1$ is true. Let $\bar{\lambda}$ be a zero of $d(\lambda)$, then we have $\Re(\bar{\lambda}) < 0$. And we can see that $\Re(\lambda_h)$ in the neighborhood of $\Re(\bar{\lambda})$ is remained by Theorem 5.1. But we cannot be certain that $\Re(\lambda_h)$ must be less than 0. We prove it in the following.

Because of $\Re(\bar{\lambda}) < 0$, there must exist a $\gamma > 0$ such that $\Re(\bar{\lambda}) \le -\gamma < 0$. Assume that there are $\Re(\lambda_h) \ge -\frac{1}{2}\gamma$, of which there exists $|d(\lambda_h)| \ge m_0 > 0$. According to Lemma 5.2, the fact $|d_h(\lambda_h) - d(\lambda_h)| \le C_1(\Lambda)h^r$ must be right; however it is contradictory with $|d_h(\lambda_h) - d(\lambda_h)| \ge m_0 > 0$. Therefore, if $R_h < 1$, then $\Re(\lambda_h) < 0$ holds. So we obtain that $U_h(t)$ is asymptotically stable.

On the other side, supposing $R_h > 1$, there must be a contradiction that makes $\Re(\lambda_h) > 0$. So, $U_h(t)$ is unstable. The proof is complete.

A.4. Proof of Theorem 6.1

Let $U_h(t) = \left(\varphi_{hi}^n, \omega_{hi}^n, \chi_h\right)^T$ be an age-semi-discrete solution of (2.7), where for $n = 0, \dots, N-1$, $i = 1, \dots, r$,

$$P_h(t) = \left(\varphi_h(t)(0), \cdots, \varphi_h(t)\left(a_r^0\right), \cdots, \varphi_h(t)(a_{N-1}), \cdots, \varphi_h(t)\left(a_r^{N-1}\right)\right),$$

$$Q_h(t) = \left(\omega_h(t)(0), \cdots, \omega_h(t)\left(a_r^0\right), \cdots, \omega_h(t)(a_{N-1}), \cdots, \omega_h(t)\left(a_r^{N-1}\right)\right),$$

$$N_h(t) = \chi_h(t).$$

Then, the row of (6.1),

$$-(P_h(t))_1 + \left(\hat{\mathcal{F}}_{1h} \frac{N_h(t)}{H + N_h(t)} P_h(t)\right)_1 = -(U_h(t)(0))_1 + \frac{2(1-f)\eta s\chi_h}{H+\chi_h} \sum_{n=0}^{N-1} h \sum_{i=1}^{r} b_i\beta_i^n (U_h(t)(a_i^n))_1 = 0,$$

$$-(Q_h(t))_1 + \left(\hat{\mathcal{F}}_{2h} \frac{N_h(t)}{H + N_h(t)} Q_h(t)\right)_1 = -(U_h(t)(0))_2 + \frac{2f\eta s\chi_h}{H+\chi_h} \sum_{n=0}^{N-1} h \sum_{i=1}^{r} b_i\beta_i^n (U_h(t)(a_i^n))_2 = 0,$$

for $n \geq 0$ and $i = 1, 2, \cdots, r$,

$$\frac{\mathrm{d}}{\mathrm{d}t}\left(P_h(t)\right)_{n(r+1)+i+1} = \frac{\mathrm{d}}{\mathrm{d}t}\left(U_h(t)\left(a_i^n\right)\right)_1 = \left(\left(\hat{\mathcal{A}}_h + \hat{\mathcal{M}}_{1h} + \hat{\mathcal{M}}_{2h}\frac{N_h(t)}{H + N_h(t)}\right)P_h(t)\right)_{n(r+1)+i+1},$$

$$\frac{\mathrm{d}}{\mathrm{d}t}\left(Q_h(t)\right)_{n(r+1)+i+1} = \frac{\mathrm{d}}{\mathrm{d}t}\left(U_h(t)\left(a_i^n\right)\right)_2 = \left(\left(\hat{\mathcal{A}}_h + \hat{\mathcal{M}}_{3h}\frac{N_h(t)}{H + N_h(t)}\right)Q_h(t)\right)_{n(r+1)+i+1},$$

$$\frac{\mathrm{d}}{\mathrm{d}t}\left(N_h(t)\right) = \frac{\mathrm{d}}{\mathrm{d}t}\left(\chi_h(t)\right) = \frac{\mathrm{d}}{\mathrm{d}t}\left(U_h(t)\left(a_i^n\right)\right)_3 = \left(\mathcal{L}_h U_h(t)\left(a_i^n\right) + \mathcal{N}_h(U_h(t)\left(a_i^n\right))\right)_3,$$

and for $n \geq 1$, denote $B^T A^{-1} E = (l_0, l_1, \cdots, l_m) \in 1 \times \mathbb{R}^{r+1}$, then

$$\mathcal{G}_h^n = \begin{pmatrix} 1 + l_0 & l_1 & \cdots & l_m \\ 0 & 0 & \cdots & 0 \\ \vdots & \vdots & & \vdots \\ 0 & 0 & \cdots & 0 \end{pmatrix} \in \mathbb{R}^{(r+1)\times(r+1)},$$

$$-\left(P_h(t)\right)_{n(r+1)+1} + \left(\hat{\mathcal{G}}_h P_h(t)\right)_{n(r+1)+1} = -\left(U_h(t)\left(a_n\right)\right)_1 + (1 + l_0)\left(U_h(t)\left(a_{n-1}\right)\right)_1 + \sum_{i=1}^{r} l_i\left(U_h(t)\left(a_i^{n-1}\right)\right)_1 = 0,$$

$$-\left(Q_h(t)\right)_{n(r+1)+1} + \left(\hat{\mathcal{G}}_h Q_h(t)\right)_{n(r+1)+1} = -\left(U_h(t)\left(a_n\right)\right)_2 + (1 + l_0)\left(U_h(t)\left(a_{n-1}\right)\right)_2 + \sum_{i=1}^{r} l_i\left(U_h(t)\left(a_i^{n-1}\right)\right)_2 = 0.$$

Hence, $P_h(t), Q_h(t), N_h(t)$ are the solutions of (6.1).

On the other hand, let $P_h(t), Q_h(t), N_h(t)$ be the solution of (6.1) and define $U_h(t) = \left(\varphi_{hi}^n, \omega_{hi}^n, \chi_h\right)^T$ by

$$\varphi_h(t)(a_n + vh) = \left(P_h(t)\right)_{n(r+1)+1} + h\sum_{i=1}^{r}\beta_i(v)\left(P_h'(a_i^n)(t)\right)_{n(r+1)+i+1}.$$

$$\omega_h(t)(a_n + vh) = \left(Q_h(t)\right)_{n(r+1)+1} + h\sum_{i=1}^{r}\beta_i(v)\left(Q_h'(a_i^n)(t)\right)_{n(r+1)+i+1},$$

$$\chi_h(t) = N_h(t).$$

Then, $\varphi_h \in \mathcal{Y}_h$ and $\omega_h \in \mathcal{Y}_h$, since for all $n \geq 0$,

$$\begin{aligned} U_h(t)\left(a_n + h\right)_1 &= \left(P_h(t)\right)_{n(r+1)+1} + h\sum_{i=1}^{r}\beta_i(1)\left(P_h'(a_i^n)(t)\right)_{n(r+1)+i+1} \\ &= \left(P_h(t)\right)_{n(r+1)+1} + B^T A^{-1} E\sum_{i=1}^{r}\left(P_h(t)\right)_{n(r+1)+i+1} = \left(P_h(t)\right)_{(n+1)(r+1)+1} = U_h(t)\left(a_{n+1}\right)_1, \end{aligned}$$

$$\begin{aligned} U_h(t)\left(a_n + h\right)_2 &= \left(Q_h(t)\right)_{n(r+1)+1} + h\sum_{i=1}^{r}\beta_i(1)\left(Q_h'(a_i^n)(t)\right)_{n(r+1)+i+1} \\ &= \left(Q_h(t)\right)_{n(r+1)+1} + B^T A^{-1} E\sum_{i=1}^{r}\left(Q_h(t)\right)_{n(r+1)+i+1} = \left(Q_h(t)\right)_{(n+1)(r+1)+1} = U_h(t)\left(a_{n+1}\right)_2, \end{aligned}$$

and $U_h(t) \in D(\mathcal{L}_h)$ since

$$
\begin{aligned}
(U_h(t)(0))_1 = (P_h(t))_1 &= \frac{2(1-f)\eta s N_h}{H+N_h} \sum_{n=0}^{N-1} h \sum_{i=1}^{r} b_i \beta_i^n \left(P_h(t)\right)_{n(r+1)+i+1} \\
&= \frac{2(1-f)\eta s \chi_h}{H+\chi_h} \sum_{n=0}^{N-1} h \sum_{i=1}^{r} b_i \beta_i^n \left(U_h(t)\left(a_i^n\right)\right)_1 ,
\end{aligned}
$$

$$
\begin{aligned}
(U_h(t)(0))_2 = (Q_h(t))_1 &= \frac{2f\eta s N_h}{H+N_h} \sum_{n=0}^{N-1} h \sum_{i=1}^{r} b_i \beta_i^n \left(Q_h(t)\right)_{n(r+1)+i+1} \\
&= \frac{2f\eta s \chi_h}{H+\chi_h} \sum_{n=0}^{N-1} h \sum_{i=1}^{r} b_i \beta_i^n \left(U_h(t)\left(a_i^n\right)\right)_2 , \\
(U_h(t)(0))_3 &= N_h(t)(0).
\end{aligned}
$$

Finally, for $a = a_i^n \in \mathcal{M}_h$,

$$
\begin{aligned}
\frac{\mathrm{d}}{\mathrm{d}t} \left(U_h(t)\left(a\right)\right)_1 &= \frac{\mathrm{d}}{\mathrm{d}t} \left(P_h(t)\right)_{n(r+1)+i+1} = \left(\mathcal{L}_h U_h(t)\left(a\right) + \mathcal{N}_h(U_h(t)\left(a\right))\right)_1 , \\
\frac{\mathrm{d}}{\mathrm{d}t} \left(U_h(t)\left(a\right)\right)_2 &= \frac{\mathrm{d}}{\mathrm{d}t} \left(Q_h(t)\right)_{n(r+1)+i+1} = \left(\mathcal{L}_h U_h(t)\left(a\right) + \mathcal{N}_h(U_h(t)\left(a\right))\right)_2 , \\
\frac{\mathrm{d}}{\mathrm{d}t} \left(U_h(t)\left(a_i^n\right)\right)_3 &= \frac{\mathrm{d}}{\mathrm{d}t} \left(N_h(t)\right) = \left(\mathcal{L}_h U_h(t)\left(a_i^n\right) + \mathcal{N}_h(U_h(t)\left(a_i^n\right))\right)_3 .
\end{aligned}
$$

Hence, $U_h(t)$ is a solution of (2.7), and the proof is complete.

A.5. Proof of Theorem 6.2

Consider the linearization form of (6.2) at $(0, 0, \sigma)^T$. Let δ_h be the eigenvalue of the first equation, and there exists $P_h \in \mathbb{R}^{N(r+1)}$ with $(P_h)_1 = 1$ such that

$$
\delta_h \left(\hat{\mathcal{E}}_h - \xi \left(\hat{\mathcal{A}}_h + \hat{\mathcal{G}}_h + \hat{\mathcal{M}}_{1h} + \hat{\mathcal{M}}_{2h} \frac{\sigma}{H+\sigma}\right)\right) P_h = \left(\hat{\mathcal{E}}_h + \xi \hat{\mathcal{F}}_{1h} \frac{\sigma}{H+\sigma}\right) P_h,
$$

that is,

$$
\left(\frac{1-\delta_h^{-1}}{\xi} \hat{\mathcal{E}}_h - \left(\hat{\mathcal{A}}_h + \hat{\mathcal{G}}_h + \hat{\mathcal{M}}_{1h} + \hat{\mathcal{M}}_{2h} \frac{\sigma}{H+\sigma} + \delta_h^{-1} \hat{\mathcal{F}}_{1h} \frac{\sigma}{H+\sigma}\right)\right) P_h = 0.
$$

According to the proof of Theorem 6.1, we have

$$
\varphi_h(t)(a_n + vh) = (P_h(t))_{n(r+1)+1} + h \sum_{i=1}^{m} \beta_i(v) \left(P_h'(a_i^n)(t)\right)_{n(r+1)+i+1} .
$$

Then, $\varphi_h \in \mathcal{Y}_h$ with $\varphi_h(0) = 1$ satisfies

$$
\hat{\mathcal{L}}_h \varphi_h = \frac{1-\delta_h^{-1}}{\xi} \varphi_h, \quad a \in \mathcal{M}_h.
$$

Therefore, we have the characteristic equation

$$d_h\left(\frac{1-\delta_h^{-1}}{\xi}\right) = 1 - \frac{2(1-f)\eta s\sigma}{H+\sigma}\sum_{n=0}^{N-1} h \sum_{i=1}^{r} b_i \beta_i^n \varphi_h\left(a_i^n, \frac{1-\delta_h^{-1}}{\xi}\right) = 0.$$

The proof is similar to the proof of Theorem 5.2.